Mineralogy and grain size variations along two carbonate margin-to-basin transects (Pedro Bank, Northern Nicaragua Rise)

John J.G. Reijmer *, Nils Andresen [1]

IFM-GEOMAR, Leibniz-Institut für Meereswissenschaften, Wischhofstrasse 1-3, D-24148 Kiel, Germany

Abstract

The analysis of nine periplatform cores in the surrounding of the Pedro Bank carbonate platform showed the presence of characteristic depositional environments during the last 300 ky. This subdivision is based on mineralogical and grain size variations in space and time.

Along the leeward, downcurrent transect the fine sediment fraction (<63 μm) dominates the periplatform sediments during interglacial highstands in sea level, and no spatial variations in the fine sediment concentration could be observed within 100 km offbank distance. The sediments are mainly of neritic origin preferentially fine aragonite needles. With increasing distance from the margin (>40 km) aragonite is still the most abundant mineral, but the percentage decreases, while the pelagic carbonate mineral content (LMC) increases. Within the subordinate coarse-fraction classes (>63 μm) the very fine sand-fraction dominates at proximal sites (<20 km) as a result of the influence of fine neritic sediments shed offbank. More distal sites (>20 km) show a more bimodal distribution pattern in the coarse grain sizes with maximum percentages within the very fine and medium sand-fraction, indicating a mixed neritic/pelagic signal.

During glacial lowstands in sea level a twofold division in the spatial distribution of the periplatform sediments is evident. A proximal environment (<28 km) with enhanced coarse-fraction percentages vs. a distal environment (>28 km) showing a strong dominance of the fine fraction (>90%). The increased coarse-fraction percentage during glacials at proximal sites results from various interacting processes: (1) lower input of fine neritic sediments, (2) increased current winnowing, and (3) redepositional processes at the upper slope during lowered sea level, and the export of this material to "proximal basinal" sites (<28 km).

At upcurrent sites the mineralogy displays a similar spatial evolution as seen along the downcurrent margin, but with overall reduced percentages. This is the result of the lower export potential of the platform against the main direction of the Caribbean Current, the most important factor for neritic sediment dispersal in the study area. The coarse-fraction content is slightly higher during interglacials compared to the downcurrent margin. During glacials a similar reduction in the percentage of the coarse-fraction is evident in a spatial context. This also substantiates the reduced sediment export and redeposition potential at the upcurrent margin.
© 2007 Elsevier B.V. All rights reserved.

Keywords: Carbonate platform; Caribbean Sea; Sea level; Carbonate export; Quaternary; Carbonate mineralogy; Grain size distribution

* Corresponding author. Current address: Université de Provence (Aix-Marseille I), Centre de Sédimentologie-Paléontologie, FRE CNRS 2761 "Géologie des Systèmes Carbonatés", 3, place Victor Hugo, Case 67, F-13331 Marseille Cédex 3, France.
E-mail addresses: John.Reijmer@falw.vu.nl (J.J.G. Reijmer), nils.andresen@mac.com (N. Andresen).
[1] Current address: ExxonMobil Upstream Research Company, P.O. Box 2189, Houston, Texas 77252, USA.

1. Introduction

In contrast to the well studied mineralogical composition of carbonate platforms and periplatform sediments, little is known about the grain size distribution and the microfacies along platform margins, although grain size analysis is a common tool in the analysis of siliciclastic sedimentary rocks. Siliciclastic sediments

are generally described using grain size, shape and/or fabric (Boggs, 1987). So far, only limited documentation has been made of these parameters for carbonate sediments. Generally it is accepted that there is a biological growth factor, which doesn't allow the use of grain size parameter to conclude for transportation processes as done in the siliciclastic realm. This study tries to substantiate that at least for modern carbonate platforms this approach is a valid tool to understand more about carbonate deposition and off-slope transportation during glacio-eustatic sea level fluctuations of the late Quaternary. Recent research on Bahamian carbonate sediments has proven the eligibility of grain size studies in the carbonate environment to trace changes in carbonate sediment production and slope development during the late Quaternary of the Great Bahama Bank (GBB) carbonate platform (Rendle and Reijmer, 2002). Rendle-Bühring and Reijmer (2005) showed the presence of distinct leeward–windward effects in grain size distribution on the margins of GBB. At the leeward margin fine sediments dominate during interglacials and coarse sediments during glacials, while the windward margin shows a reversed pattern with coarser sediments in interglacials and finer sediments in glacials.

The main objective of this study was to gain insight into the export pattern of the inclined Pedro Bank carbonate platform by using grain size variations and mineralogy in combination with the microfacies of the periplatform sediments to differentiate depositional environments as well as depositional processes in this modern carbonate environment.

2. Dataset and methods

2.1. Dataset

Nine sediment cores from the periplatform environment around Pedro Bank were analyzed. Cores were taken from water depths ranging from 648 to 2520 m with offbank distances ranging from 5.5 to 91 km (see Table 1 and Fig. 1).

Six cores are located along the northwestern margin of Pedro Bank forming a platform-to-basin transect on the downcurrent side of Pedro Bank. The other cores (7–9; Fig. 1) were recovered from the southwestern to southeastern margin and are used to show sedimentation processes present along the upcurrent margin. For the mineralogical and sedimentological analysis of the nine cores (Table 1), 602 sediment samples were analyzed. They were sampled at 10 cm spacing within the individual cores.

2.2. Methods

The following methods were used in this study: (1) stratigraphical analysis: oxygen isotope analysis of *Globigerinoides sacculifer*, U/Th-dating of marine bulk sediment, AMS ^{14}C-dating of mixed Holocene and Marine Isotope Stage 3 (MIS 3) coarse-fraction samples (Fig. 2), (2) determination of calcium carbonate content of the fine fraction and bulk sediment, (3) X-ray powder diffraction of the fine fraction to determine the carbonate mineralogical composition of sediments, and (4) grain size analysis (Fig. 3).

Interglacial and glacial percentages are averaged for each core for mineralogy, the content of coarse vs. fine fraction and the grain size subfractions. Marine oxygen isotope stages 2, 3 and 4 have been, where possible, separated in the stratigraphy. Interstadial MIS 3 is thought to have had sea level stands of up to 40 m below present day sea level (Chappell et al., 1996), which would result in the flooding of small areas around the southward inclined top of Pedro Bank. Therefore we aimed to separate the percentages for this interstadial stage, to exclude them from calculations of interglacial and glacial mean percentages. Interglacial and glacial mean percentages are

Table 1
Core location, relative position, water depth and core length of the nine analysed sediment cores from the periplatform environment surrounding Pedro Bank

| No. in Fig. 1	Core no.	Relative position (closest distance to active bank margin)	Down-/upcurrent position	Position latitude (°N)	Position longitude (°W)	Water depth (m)	Length of core (cm)
1	M35048-1	NW-Transect (5.5 km)	Downcurrent	17.6469	78.9144	648	517
2	M35049-2	NW-Transect (19.5 km)	Downcurrent	17.6438	79.0877	893	513
3	M35043-1	NW-Transect (28 km)	Downcurrent	17.6441	79.1691	975	431
4	M35042-2	NW-Transect (41 km)	Downcurrent	17.6486	79.3094	1023	556
5	PC 059	NW-Transect (72 km)	Downcurrent	17.7255	79.6353	1887	571
6	PC 100	NW-Transect (91 km)	Downcurrent	17.9211	79.7166	2520	519
7	M35034-1	SW-Edge (10 km)	Upcurrent	16.9092	79.0694	1211	231
8	M35032-2	SW-Edge (25 km)	Upcurrent	16.5925	78.6261	1364	354
9	M35052-2	SE-Edge (30 km)	Upcurrent	16.5753	77.7028	1445	965
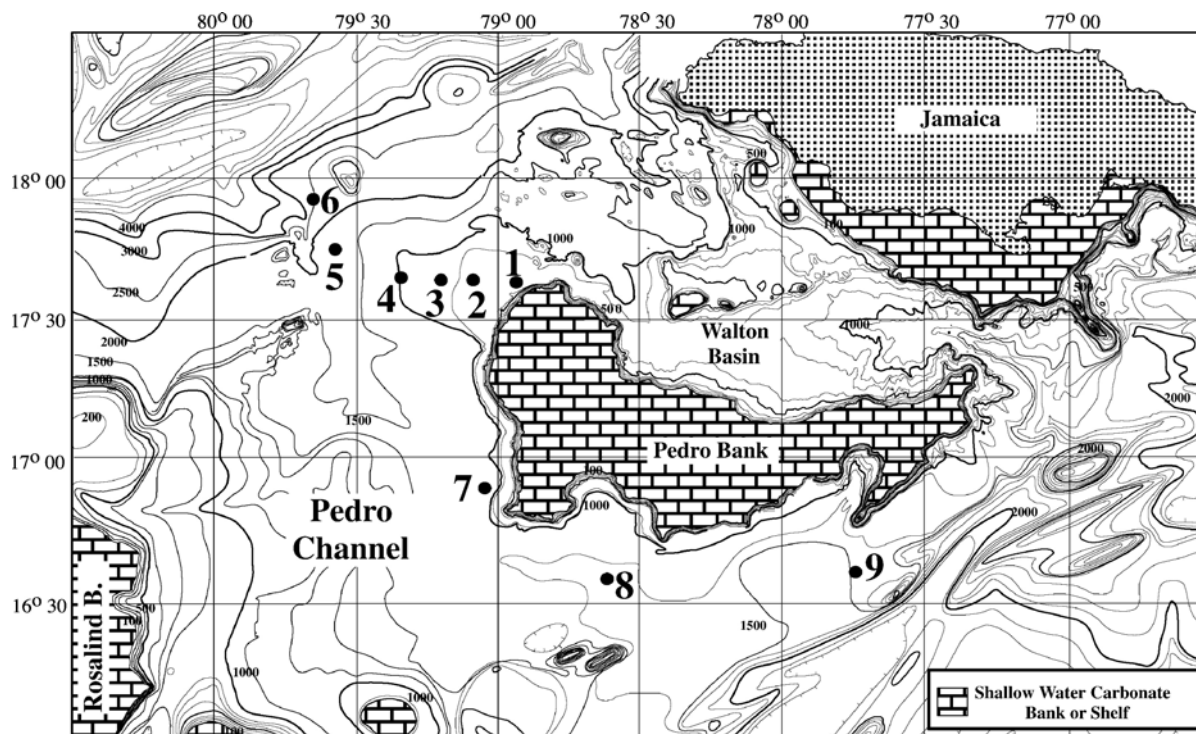
Fig. 1. Bathymetric map for Pedro Bank area with core locations. Bathymetry is based on revised data collected during several American research cruises to the Northern Nicaragua Rise (modified after Cunningham 1998). Core abbreviations: 1 = M35048-1; 2 = M35049-2; 3 = M35043-1; 4 = M35042-2; 5 = PC059; 6 = PC100; 7 = M35034-1; 8 = M35032-2; 9 = M35052-2).

shown with increasing offbank distance, which also accounts for increasing water depths.

In addition, characteristic data for each site will be shown for a variety of specific proxies (e.g. fine aragonite content or the weight percentage of the 125–250 μm) versus time or depth to show the temporal changes of single sediment proxies.

A detailed description of the methods, including detailed information on the stratigraphic framework (Fig. 2) and the sediments analysed (Fig. 3), is given in Appendix A.

3. Results

3.1. Temporal variations of mineralogical proxies

3.1.1. Downcurrent transect

The most shallow and proximal site 1 shows a clear shallow-water (platform) input signal with high percentages of fine aragonite in the bulk sediment (60–80%) during interglacials (sea level highstands) and lower percentages (30–40%) during glacial periods (Fig. 4A). The maximum percentage of HMC increases for each younger consecutive interglacial towards the core top. The LMC content decreases from MIS 8 to the present

(maximum percentage about 25% during early MIS 7). Quartz intensities in the fine fraction vary little during glacial and interglacial intervals.

Sediment cores 2–4 from intermediate water depths (893–1023 mbsl) and offbank distance (19–42 km) show similar percentages of aragonite, with higher contents in interglacials (50–70%), whereas glacial periods display lower percentages between 20–30% (Fig. 4B–D). The content of HMC steadily increases further downslope. The percentage of HMC is lower during interglacial and higher during glacial periods, with maximum percentages during late MIS 6. At all sites LMC generally peaks during glacial times, and shows low percentages during interglacial periods. Quartz shows relative high intensities during glacial MIS 2–4, 6 and 8 and small amplitudes characterize interglacials. The intensity of quartz in general mirrors the content of fine non-carbonates (Andresen, 2000).

Although the sediments at deep (1887–2520 mbsl) and distal (72–92 km) sites 5 and 6 were deposited in depths exceeding 1800 mbsl (Fig. 4E and F). Interglacials are characterized by higher percentages of aragonite (30–55%), whereas glacials show lowest percentages between 5–25%. The HMC content in core 5 shows higher percentages during glacial than during interglacial periods.
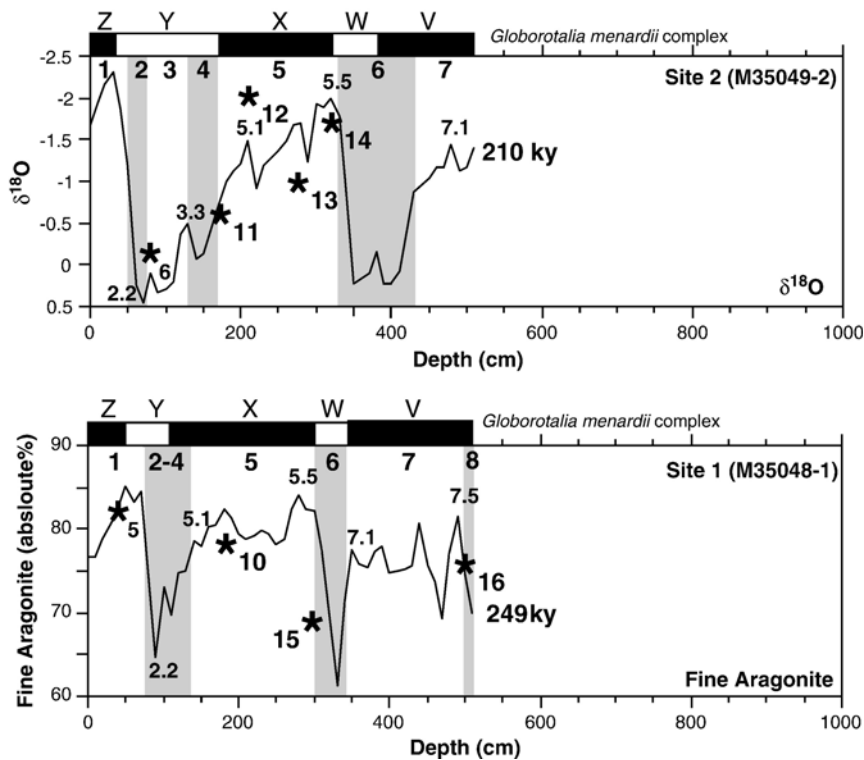
Fig. 2. Stratigraphy of two selected cores. Upper graph shows oxygen isotope stratigraphy for core 2. Lower graph shows aragonite stratigraphy for core 1. Grey shaded area marks glacial periods. At the top of each graph letters and shaded rectangles mark the *Globorotalia menardii* complex, a biostratigraphic tool. Numbered asterisk mark AMS14C or 230Th/238U-ages: *5=7160±40 yr; *6=43390±1540 yr; *10=91±10 ky; *11=83±34 ky; *12=94±29 ky; *13=104±29 ky; *14=172±16 ky; *15=120±6 ky; *16=225±12 ky.

Both deep sites 5 and 6 show a decrease in the percentage of LMC from the end of MIS 8 towards the recent. Higher percentages of LMC (30–50%) are present in glacial periods (MIS 6 and 8), whereas interglacial LMC contents vary between 10–30%, with lowest percentages during the Holocene. The content of fine non-carbonates and the quartz both show the same trends with highest percentages in glacials and interglacial MIS 7.4.

3.1.2. Upcurrent sites

The temporal changes within upcurrent sediment cores from intermediate water depths will only be described in detail for site 9 (Fig. 5C). Core 7 (Fig. 5A) recorded only a limited time slice from the early MIS 3 to the Holocene, whereas the stratigraphy for site 8 (Fig. 5B) is interrupted by numerous turbidite layers hampering a proper interpretation.

The content of fine aragonite, predominantly aragonite needles, in the bulk sediment of site 9 (Fig. 5C) displays a relatively clear "highstand shedding pattern" with 25–30% fine aragonite during interglacial MIS 1, 3 and 5, and 10–15% during glacial MIS 2, 4 and 6. The percentages found are clearly lower than those observed on the down-

current side of Pedro Bank. The percentage of fine aragonite during interglacials shows a decreasing trend from MIS 1 to 9. The HMC percentage at site 9 generally displays higher percentages during glacials and during MIS 3. The LMC percentage shows an overall decreasing trend from MIS 9 to MIS 1, but no clear link with glacial/interglacial periods. The intensity of fine quartz and of fine non-carbonates show low intensities at the beginning of interglacials with an increasing trend towards the next glacial, and a generally decreasing trend from middle of MIS 3 towards the recent.

3.2. Temporal variations of single grain sizes

The periplatform sediments retrieved from the slopes and deep basins off Pedro Bank show a dominance by planktic foraminifera (*Orbulina*, *Globigerina*, *Rotaliida* and *Globigerinida*) and pteropods within the 500–1000 μm and >1000 μm-fraction (Fig. 3). In certain coarse-fraction samples of the "proximal" downcurrent cores M35048 and-49 an enrichment of peloids could be observed. The "finer" coarse-fractions (i.e. 63–125 μm, 125–250 μm and 250 μm) show generally a high
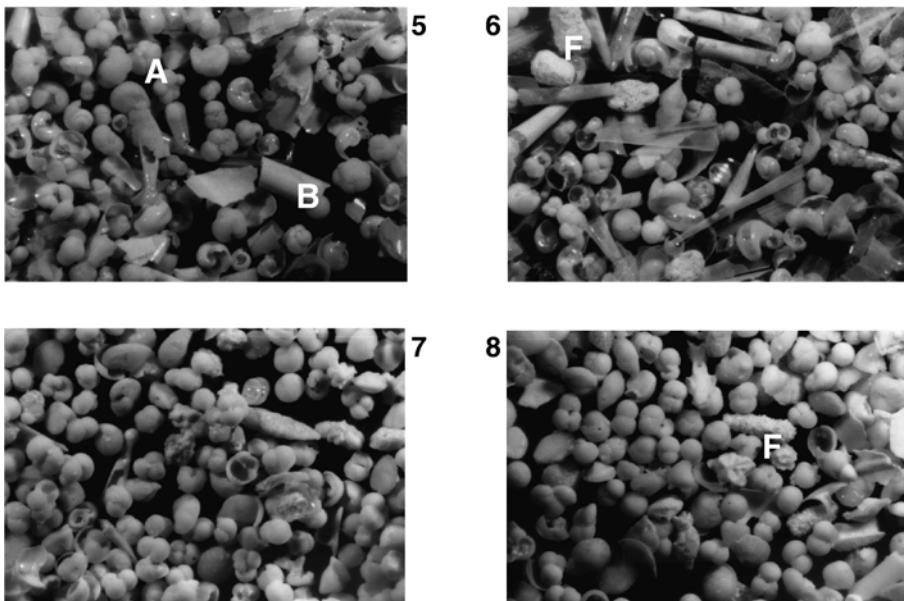
Interglacial
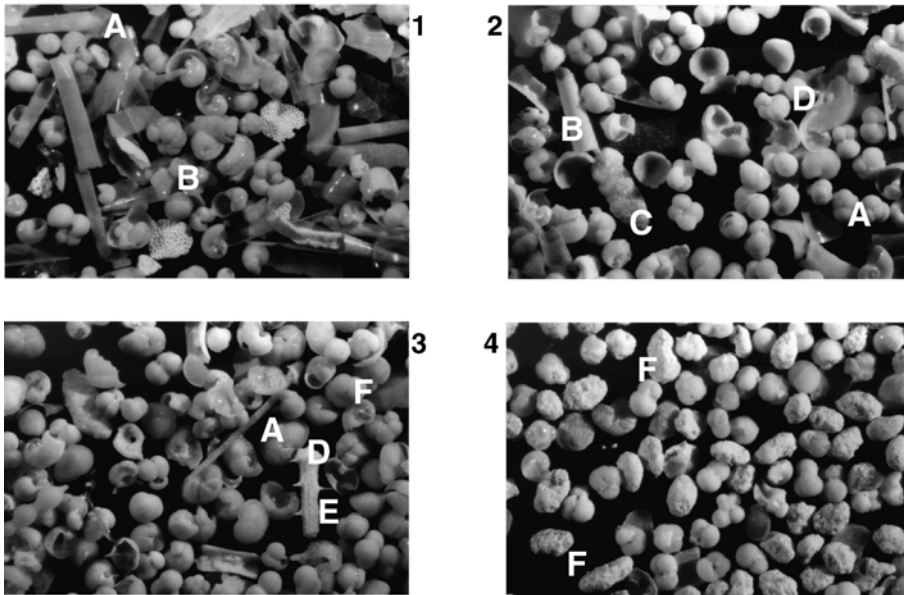
Glacial

Fig. 3. Selected micro-photographs of interglacial (upper four photos) and glacial (lower four photos) coarse-fraction samples. Magnification is 84×, scale across each photo approx. 0.9 mm, and the subfraction shown is 250–500 μm or 355–425 μm. 1 = Core 8, 330 cm, 2 = Core 1, 390 cm, 3 = Core 1, 230 cm, 4 = Core 1, 190 cm, 5 = Core 8, 180 cm, 6 = Core 7, 130 cm, 7 = Core 1, 330 cm, 8 = Core 1, 510 cm. A = Planktic foraminifera, B = Pteropods, C = Miliolid foraminifera, D = Nodosaria sp., E = Echinoderm spines, F = Peloids (preferentially in proximal cores).

content of small planktic foraminifera, as well as peloids and pteropod fragments. Benthic foraminifera and shallow-water derived biota are present in very minor amounts (Andresen, 2000).

3.2.1. Downcurrent transect

At proximal site 1 (Fig. 4A) high percentages of coarse-fraction are observed during glacial periods (peaks of 40–50%). Another general trend is a slight

coarsening upward sequence within each interglacial. The fine fraction (<63 μm) shows highest percentages during interglacials and almost mirrors the single events of the aragonite content. The very fine sand-fraction dominates during interglacial times with maximal percentages of 60%, whereas during glacial MIS 2 and 6 lowest percentages (15–20%) are found. The fine sand-fraction shows major peaks in conjunction with marine isotope stage boundaries, preferentially during transgressive phases in sea level. The very coarse sand-

fraction shows similar percentages of about 2.5% during interglacials and glacials.

Intermediate distance sites 2 and 3 (Fig. 4B, C) show a very similar temporal trend in the coarse-fraction distribution with a long-term increase from the base of each core towards the Last Glacial Maximum. No general glacial/interglacial cyclicity is observed, but major changes (of about 15–20%) occur near MIS boundaries. The 63–125 μm-fraction in core 2 shows no clear glacial–interglacial cyclicity, but high abundances during
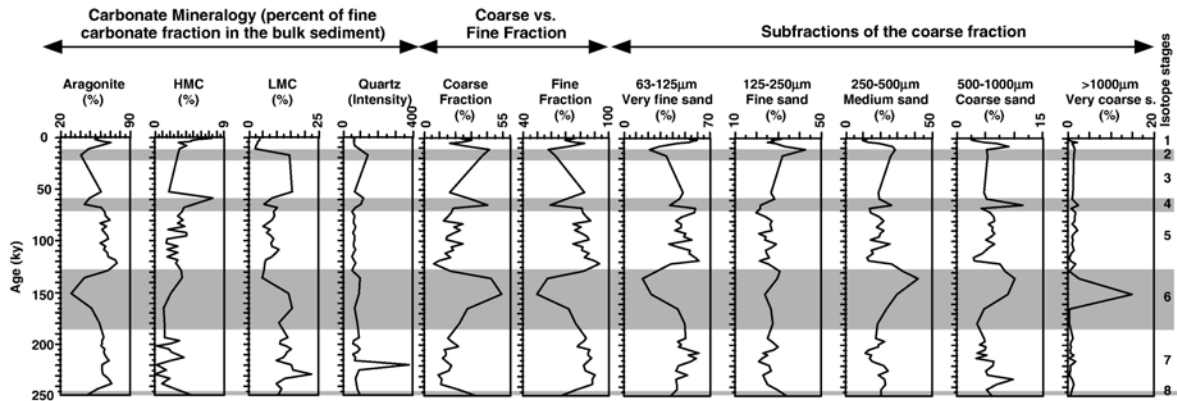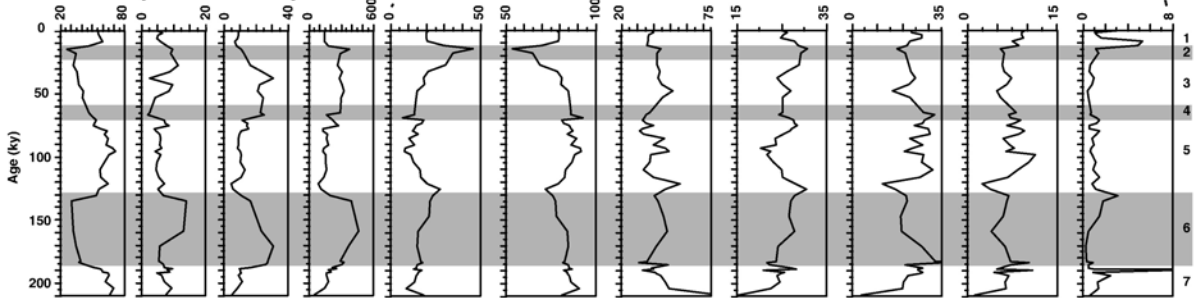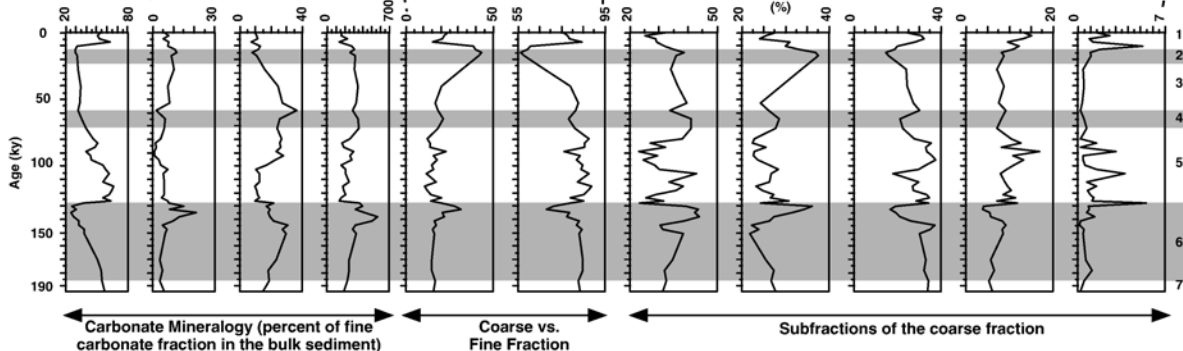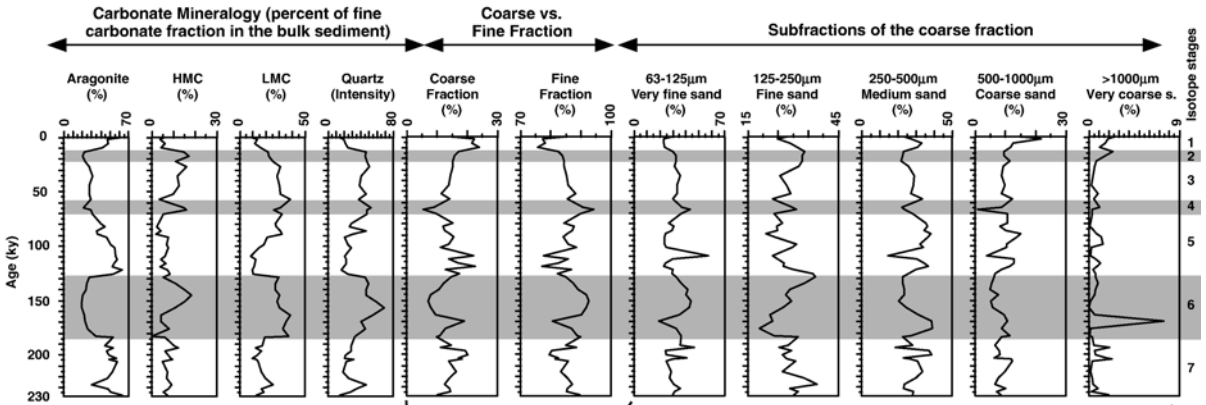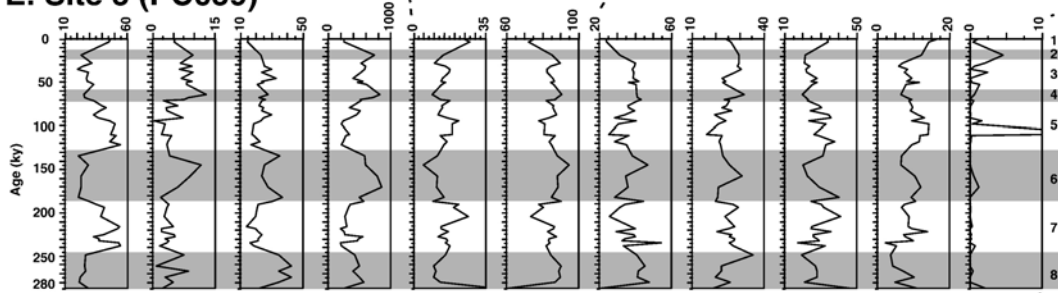

Fig. 4. Temporal variations of mineralogical and grain size proxies at (A) downcurrent Site 1, (B) Site 2, (C) Site 3, (D) Site 4, (E) Site 5, and (F) Site 6. Grey shaded areas indicate glacial marine oxygen isotope stages (MIS).
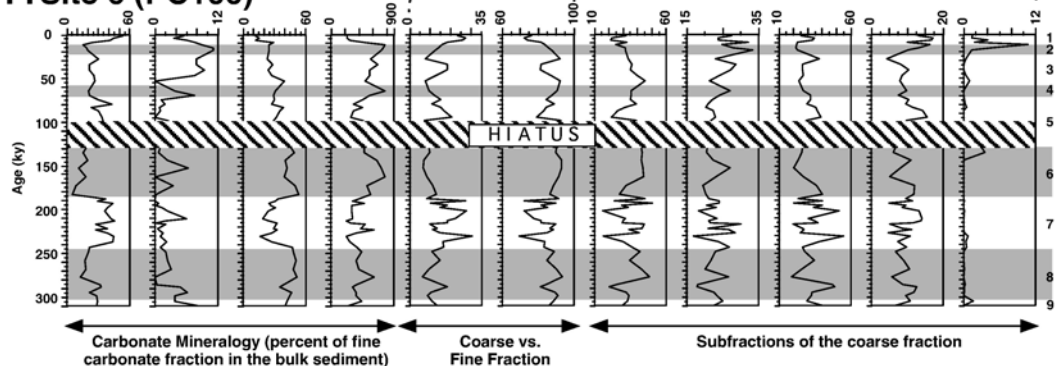
Fig. 4 (*continued*).

interglacial MIS sub-events (see Fig. 4B). This trend is not present in core 3, which only shows maxima in the very fine sand-fraction during glacial MIS 2, 4 and late MIS 6. Temporal changes of the fine sand-fraction (125–250 μm) at site 3 mirror those seen for the very fine sand-fraction.

At site 2 the medium and coarse sand-fraction contents are higher in interglacials and lower in glacials and MIS 3. Intervals close to stage boundaries display distinct changes (see MIS 7/6 or 6/5 boundary). At site 3 increased percentages of fine sand occur at the very

beginning of MIS 5 (probably within the transgression) and a high medium sand content is present during early MIS 6, whereas the 500–1000 μm-fraction shows overall minimum percentages. The percentage of the very coarse sand-fraction shows distinct peaks at both sites along the MIS 2/1 and 6/5 transgression and several maxima (3–4%) within MIS 5 at site 3.

The temporal variability of the coarse-fraction within the three distal sites 4, 5 and 6 (Fig. 4D–F) displays lower percentages during glacial periods, whereas higher percentages and also a higher variability is evident during
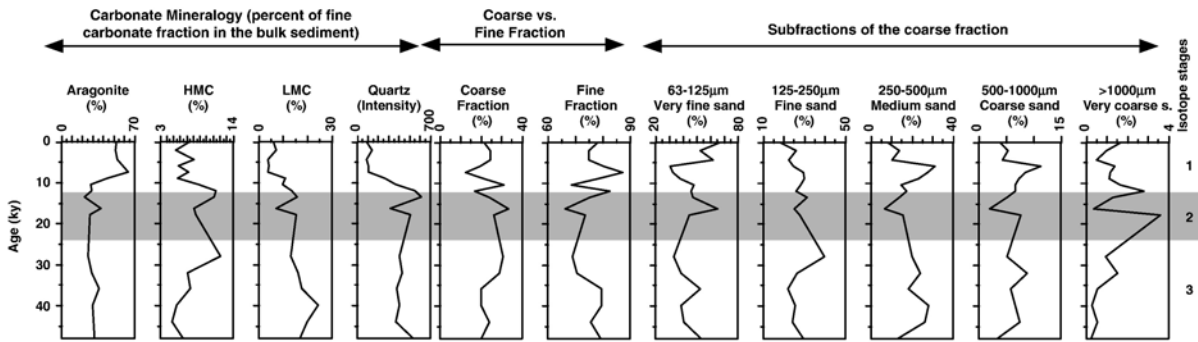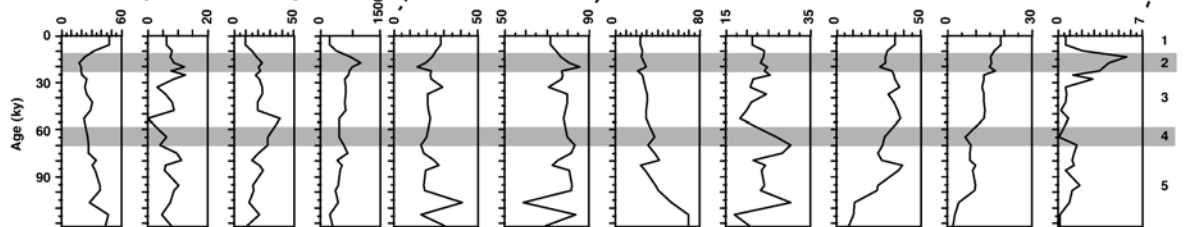
Fig. 5. Temporal variations of mineralogical and grain size proxies at upcurrent (A) Site 7, (B) Site 8 and (C) Site 9. Grey shaded areas indicate glacial marine oxygen isotope stages.

interglacial times. Interglacial percentages vary between 15–30%, those for glacials between 5–15%. The fine fraction content shows highest percentages during glacial MIS 4, 6 and 8 and around MIS event 3.1 in core 5 and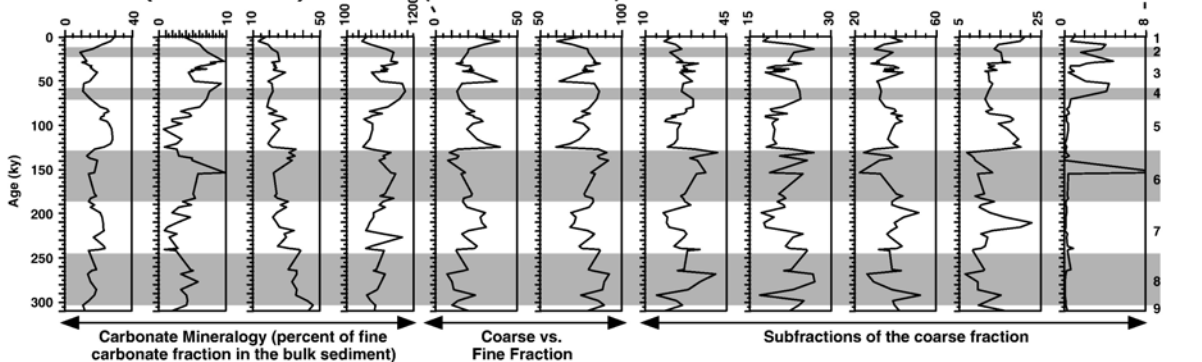 6. At these three distal sites 4–6, the very fine sand-fraction displays slightly raised percentages during glacials (Fig. 4D–F). The same holds for the coarse and very coarse sand subfraction. The 250–500 µm-fraction shows distinct peaks at all sites (around 100 ky, 120 ky, early MIS 6 (170–180 ky), 200–210 ky and 280–290 ky).

3.2.2. Upcurrent sites

The temporal changes are only described in more detail for site 9 (Fig. 5C). Sites 7 and 8 do not provide

detailed information with enough temporal resolution (Fig. 5A–B). The temporal variations in the coarse-fraction content of site 9 mirrors the marine oxygen isotope curve peaking during interglacial events and low percentages during glacials (MIS curve not shown for every core). The single subfractions, the 63–125 µm and 125–250 µm-fraction, show very similar trends to those described for the fine fraction, whereas the 250–500 µm and 500–1000 µm-fraction mirrors the trend displayed by the coarse-fraction content. The very coarse sand-fraction content is generally lower than 2% besides 4 major maxima of 4–10% occurring during glacial MIS 2, 4 and at MIS event 6.4 (151 ky).

3.3. Spatial variations in mineralogy along platform-to-basin transects

3.3.1. Downcurrent transect

During interglacials the aragonite content decreases continuously (64–36%) with increasing distance and water depth along this transect. LMC increases from on average 8.5% in proximal sites to 30% at distal site 6. Mid-distanced sites 3 and 4 contain similar percentages of LMC (±15%). HMC varies between 3.3% in the most proximal site to slightly raised percentages of 5.5–6.5% for sites located between 20–42 km offbank distance or 893–1023 mbsl. Further downslope (1887–2520 mbsl) the average HMC percentage decreases again to values
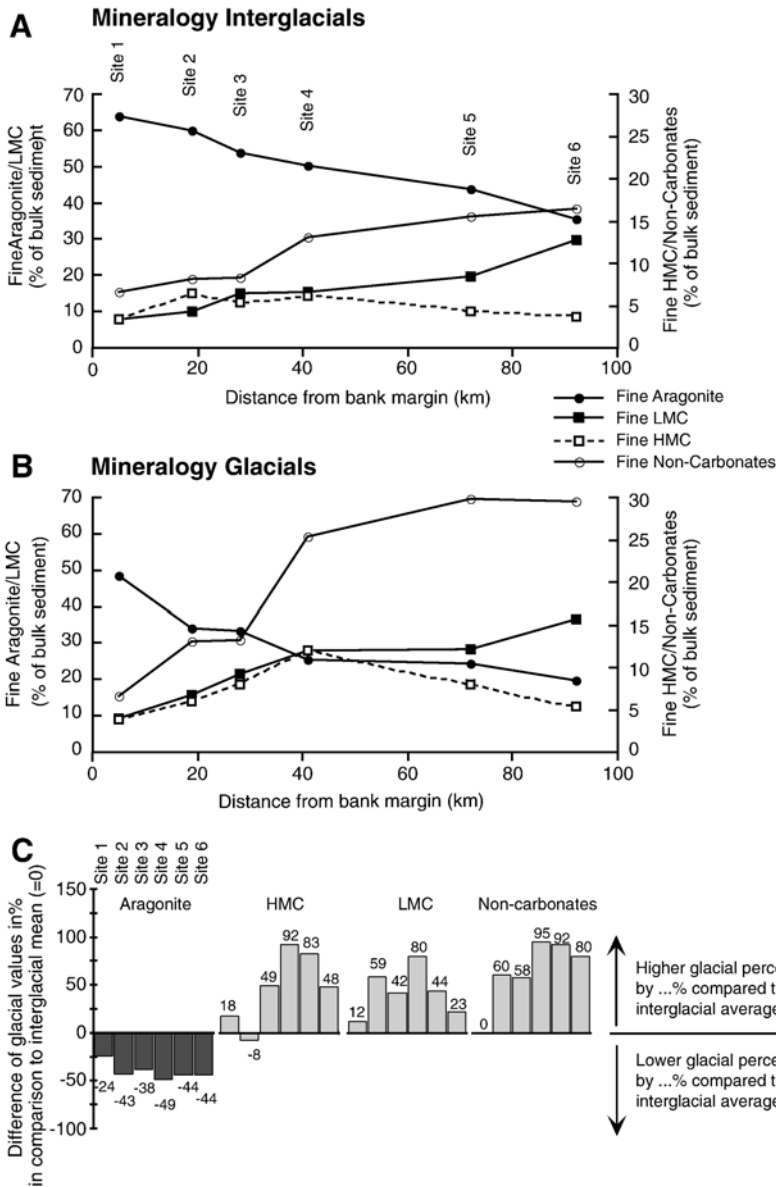
Fig. 6. (A) and (B). Spatial mineralogy distribution along northwestern offbank transects. Mineral content shown is calculated fine fraction mineral percentage within the bulk sediment (see Methods for calculation). (C) Percentual interglacial-to-glacial comparison. Positive numbers show higher glacial percentage compared to the interglacial mean, a negative number shows a lower percentage. Aragonite as indicator for neritic export to the basin shows reduced glacial input along the entire transects. HMC displays a bimodal distribution with little change at proximal sites and largest glacial-to-interglacial differences at mid-distanced site 4. LMC and non-carbonates show clearly enhanced percentages during glacial along the entire transect, but lowest differences for most proximal site 1, which is probably influenced by current winnowing.

of approx. 3.5%. The content of fine non-carbonates displays a constant increase with increasing water depth and offbank distance (6.5–16.5%).

During glacials the most proximal site 1 contains high percentages of aragonite (up to 49%). Sites 2 and 3 (20–28 km offbank distance) show nearly identical aragonite percentages of 34%, as well as sites 4 and 5 further downslope (25%). The minimum percentage is found at the most distal site 6 with 20% aragonite on average during glacials. The LMC percentage in glacial periods is generally higher than during interglacial periods. LMC increases downslope (10–38%), with sites 4 and 5 showing an almost identical mean percentage (28%), although they differ by 40 km distance or 800 m water depth. The mean HMC content is in general higher during glacial periods, although the difference between interglacials and glacials at sites 1 and 2 is negligible. The most obvious increase in the glacial HMC content is evident at site 4 (1023 mbsl), where the average HMC content increases from 6.2% to 12%. The most distal and deepest sites
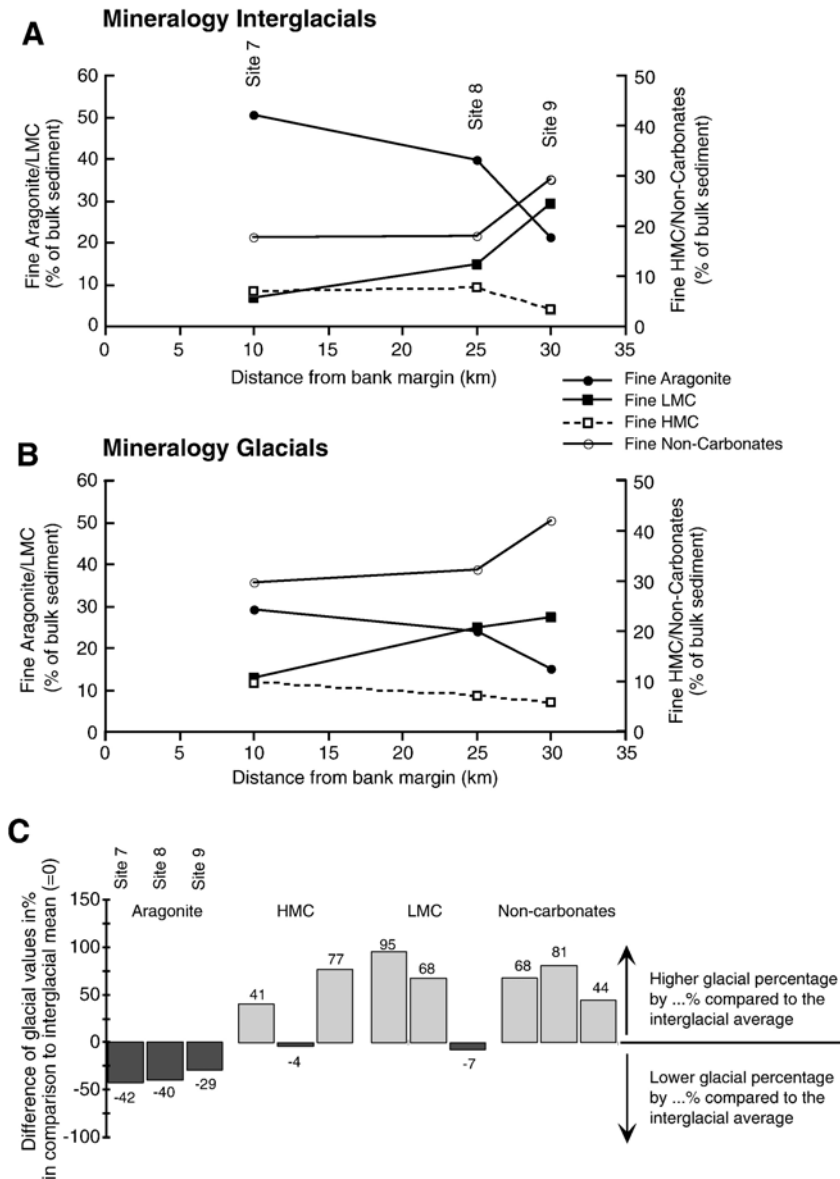
Fig. 7. (A) and (B). Spatial mineralogy distribution of upcurrent periplatform sites. For further explanation on (C) refer to caption Fig. 6C. Although the cores do not display a real offbank transect, they still show the decreasing influence of neritic export and increasing influence of pelagic and terrigenous sediment components with greater offbank distance. Data for site 8 must be treated with care, as this core is disturbed by turbidites.

5 and 6, display again lowered percentages of HMC (Fig. 6). The percentage of fine non-carbonates increases along the entire transect, except for proximal site 1, which shows only minor differences in interglacial and glacial percentages of non-carbonates.

3.3.2. Upcurrent sites

During interglacials the average content of fine aragonite in bulk sediment shows a constant decrease with increasing offbank distance/water depth (51–21%). Highest percentages were found at the most proximal site 7 (10 km offbank distance) and correlate with the percentages at downcurrent site 4 (offbank distance 41 km). At the most distal site 9, about 21% fine aragonite is found on average during interglacials. This is about 3/4 less on an absolute scale than for most distal site 6 on the down-

current margin. LMC also displays a continuous increase with increasing offbank distance, varying between 7–30% during interglacials. The percentage of HMC during interglacials averages about 7% within the southwestern, proximal located sites 7 and 8, whereas distal site 9 only shows an average interglacial percentage of 3.5%. Fine non-carbonates vary between 17% for southwestern sites 7 and 8, and show a maximum interglacial average percentage of nearly 30% at site 9. These percentages are higher than maximal percentages along the downcurrent transect in interglacials.

During glacial periods the mineralogy of periplatform sediments along the upcurrent margin of Pedro Bank shows the following characteristics: average percentages of fine aragonite decrease (29–15%) with increasing offbank distance/water depth. This equals an
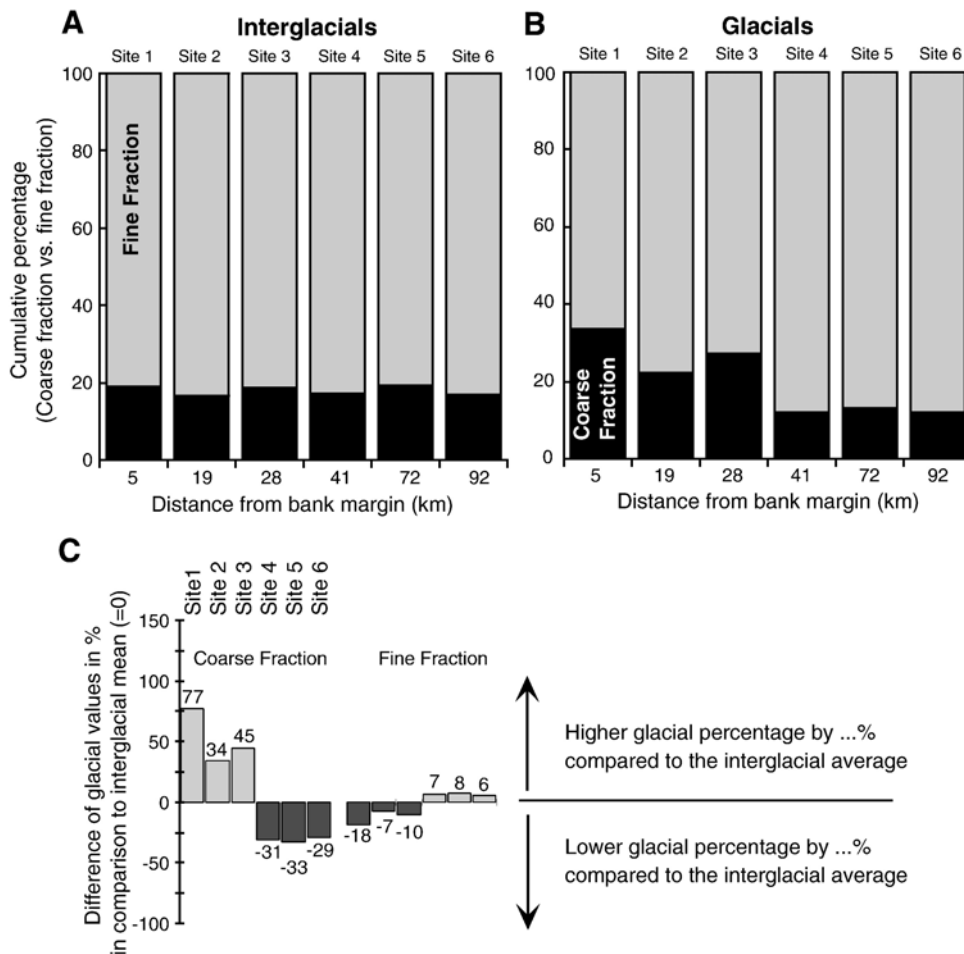
Fig. 8. (A) and (B). Spatial coarse vs. fine fraction distribution along the northwestern offbank transect. For further explanation on figure (C) refer to caption Fig. 6C. During interglacials no major changes in the content of coarse and fine fraction occurs along the entire offbank transect. Glacial periods, however, show two distinct environments. Cores 1 to 3 (within <28 km offbank distance) display raised glacial coarse-fraction contents (see lower figure), which might be the result of lower input of fine neritic components, current winnowing and/or redepositional processes. More distal sites show a very similar coarse vs. fine fraction pattern, which might reflect a more homogenous open ocean sedimentation.

interglacial-to-glacial reduction in the aragonite contents of one-third to a half (Fig. 7). The content of fine LMC shows lowest percentages in proximity of the platform (13% in core 7), whereas sites 8 and 9 show very similar percentages of about 25–27%. The content of LMC in glacials is clearly higher than in interglacial periods at sites 7 and 8, whereas most distal site 9 shows very similar percentages of LMC during glacials and interglacials. The average content of HMC shows a continuous decrease with increasing water depth (9% to 6%; Fig. 7A and B) at upcurrent sites. The percentage of fine non-carbonates during glacials in the southern sites increases from about 30% in site 7 to a maximum of 42% at site 9 (Fig. 7). The input of non-carbonates is therefore about twice as high during glacial as during interglacial times (44–81%; Fig. 7).

3.4. Spatial grain size variability along platform-to-basin transects

3.4.1. Coarse vs. fine fraction in downcurrent transect

At the studied sites the percentage of fine fraction varies between 76% and 85%. Independent from up- or downcurrent location the lowest fine fraction contents are found at proximal sites 1 and 7. In general, the fine fraction content along the downcurrent side is slightly higher (79–85%) than at upcurrent sites (76–80%).

During interglacials the proportion of the coarse and fine fraction along the northwestern transect does not show any significant variations. The coarse-fraction varies between 17% and 19% with highest percentages at sites 1, 3, and 5. During glacial times the sites along the transect can be subdivided into three different
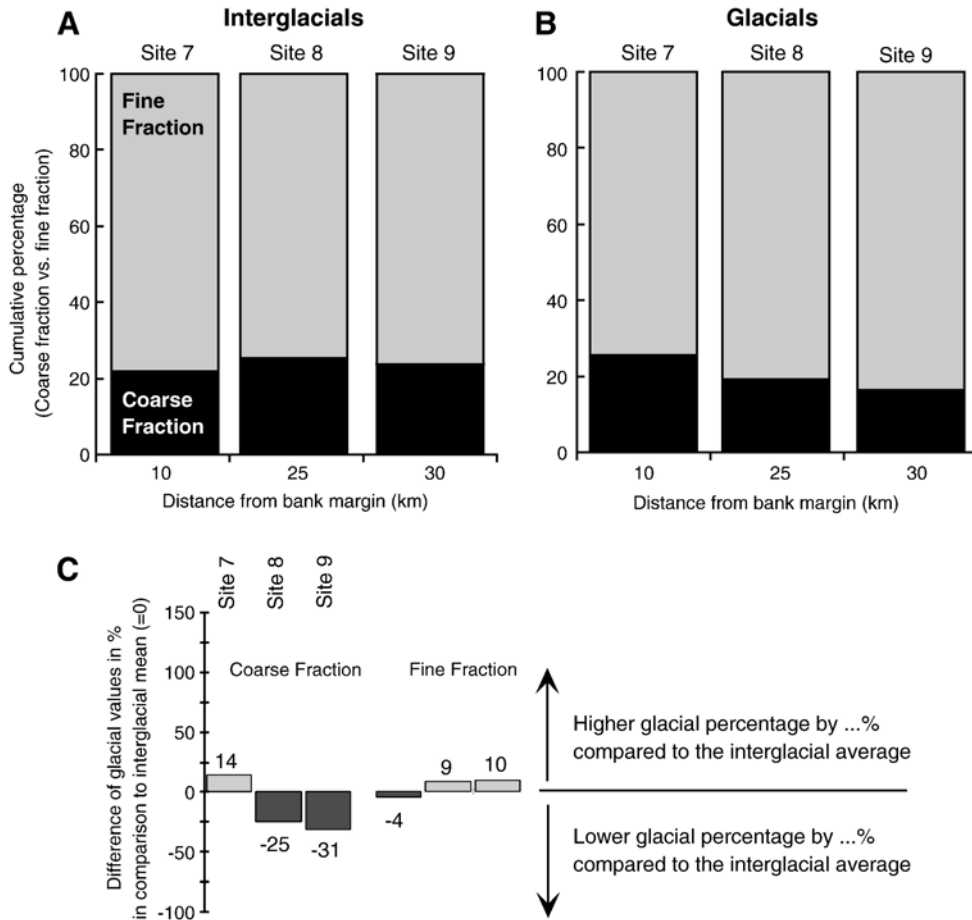
Fig. 9. (A) and (B). Spatial coarse vs. fine fraction distribution of upcurrent periplatform sites. For further explanation on figure (C) refer to caption Fig. 6C. The interglacial content of coarse and fine fraction is very similar in all analysed upcurrent sediment cores, displaying no real trend. During glacials a decrease in the coarse-fraction content can be observed. Higher percentages at the most proximal site might indicate a stronger influence of redeposited material closer to the slopes of Pedro Bank. Higher coarse-fraction content at proximal site 7 may be the result of enhanced current activity, resulting in winnowing of fine sediments.

depositional environments. At most proximal site 1 14% more coarse-fraction was deposited during glacials, whereas sites 2 and 3 show a minor increase of only 5.5% and 8%, respectively, in comparison to their average interglacial percentages (Fig. 8A and B). In contrast, at downslope sites 4, 5, and 6 about 5–6% less coarse-fraction was deposited. This trend is also apparent when looking at the glacial-to-interglacial difference of the coarse-fraction content (Fig. 8C). At site 1 about 77% more coarse-fraction is recorded during glacials in comparison to the interglacial mean (Fig. 8C). Sites 2 and 3

show "only" 34–45% more coarse-fraction, whereas sites 4, 5, and 6 show a very similar reduction of about 29–33% less coarse-fraction in glacial periods (Fig. 8C).

3.4.2. Coarse vs. fine fraction in upcurrent sites

Similar to the downcurrent transect, the interglacial coarse and fine fraction content within the upcurrent sites shows minor changes, which are independent from their relative position to the platform edge (22.2–25.3% respectively 77.8–74.7%). The absolute coarse-fraction percentage, however, is higher by about 6% in
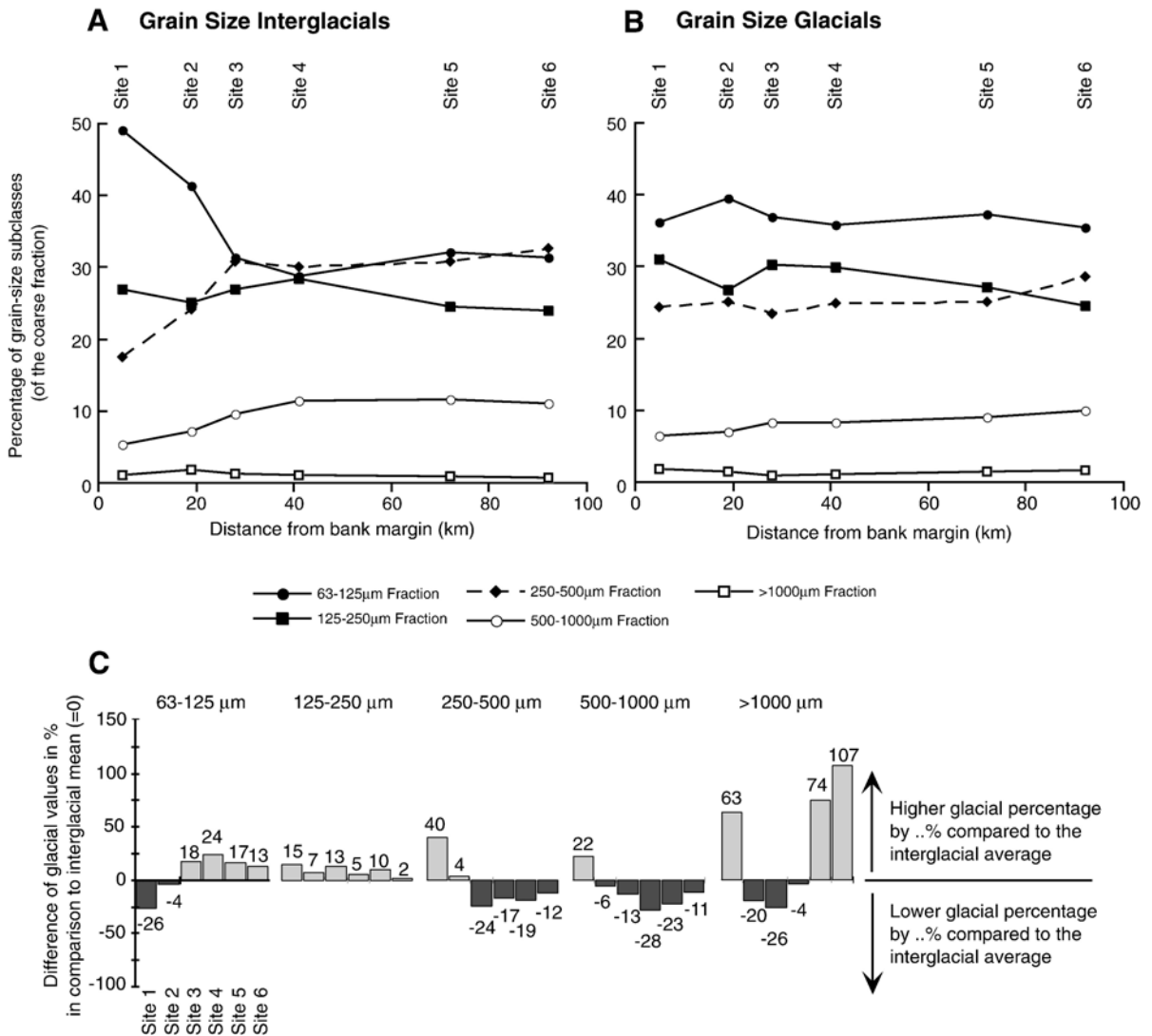
Fig. 10. (A) and (B). Spatial subfraction distribution pattern along northwestern offbank transects. Percentages shown are percent of the coarse-fraction. For further explanation on the figure (C) refer to caption Fig. 6C. During interglacials sediments at proximal sites are mainly composed of fine neritic sediment material from the bank top. This is shown by their highest percentages in very fine to fine sand-fraction ("normal" sorting pattern). The pelagic influence becomes evident through a more bimodal grain size distribution pattern with increasing distance, showing maxima in very fine (neritic signal) and medium sand-fraction (pelagic signal). During glacials normal sorting is evident with a decrease of each consecutive coarse grain size class.

comparison to the downcurrent margin. Along the upcurrent side of Pedro Bank the tendency of highest coarse-fraction percentages in proximal sites and a decreasing trend with increasing offbank distance also can be observed during glacial periods. The proximal site 7 shows a coarse-fraction content of about 25%, which is lower than the 33% found in the most proximal site 1 on the downcurrent margin. Sites 8 and 9 reveal coarse-fraction percentages between 16–19% (Fig. 9), which is lower than those observed at a similar distance along the downcurrent margin (Fig. 8). Only proximal site 7 exhibits a minor increase by 14% compared to averaged interglacial contents, whereas 8 and 9 show a similar decrease of 25–31% in the percentage of coarse-fraction (Fig. 9C).

3.4.3. Coarse-fraction subfractions in downcurrent transect

During interglacials the most proximal site 1 shows a strong dominance of very fine and fine sands (together more than 75%), and a gradual decline to coarser subfractions, thus displaying a negative skewness within the coarse subfractions. With increasing offbank distance the distributional pattern within interglacials becomes more bimodal, as subfractions such as the very fine and medium sands occur more frequently. The very fine sand-fraction shows a continuous decrease (50–29%) along sites 1 to 4 situated on the relatively flat submarine plateau on the northwestern margin (Fig. 10A; see also bathymetry in Fig. 1), whereas sites 5 and 6, located on the flanks of Pedro Channel, show similar percentages
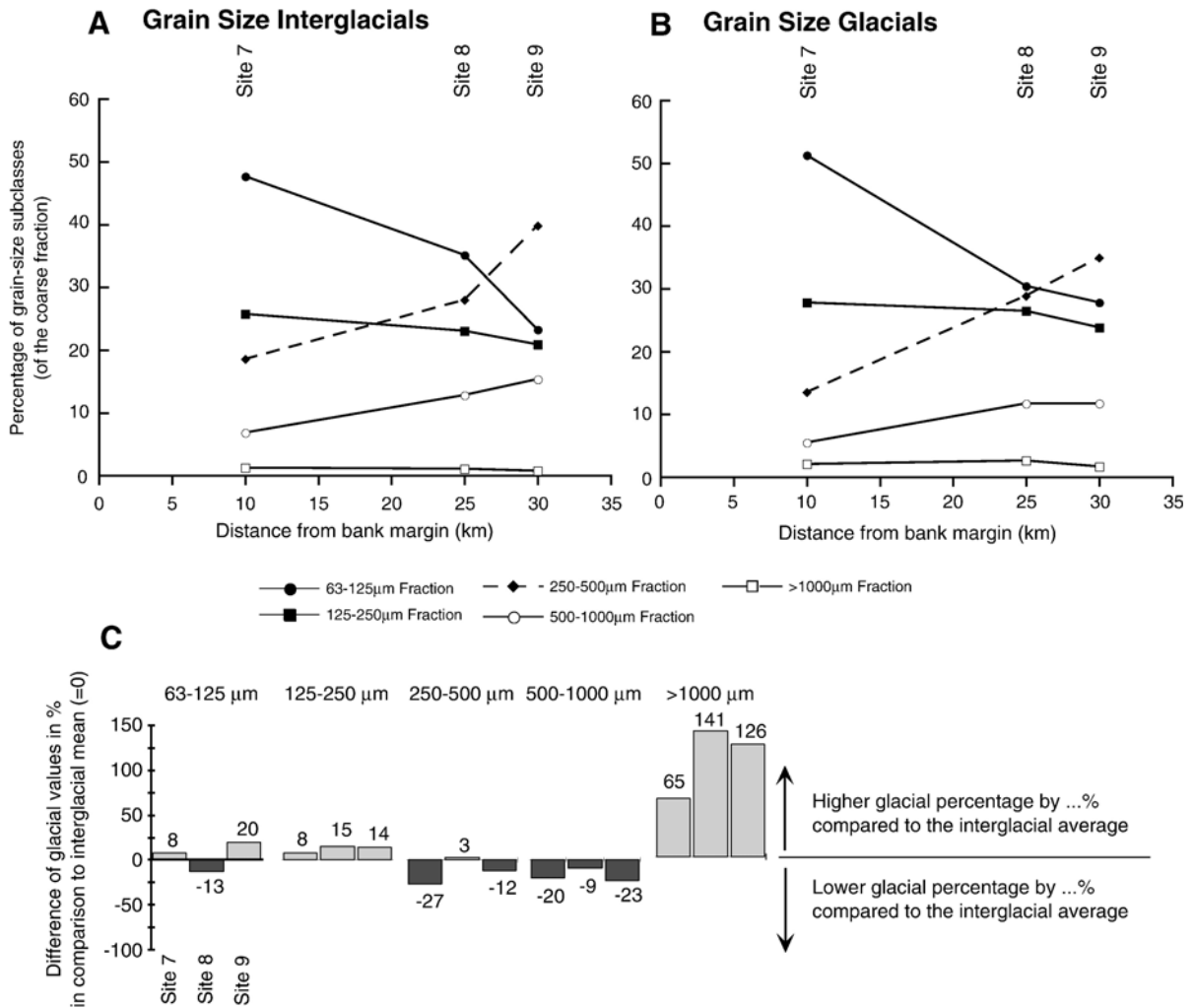
Fig. 11. (A) and (B). Spatial subfraction distribution pattern of upcurrent periplatform sites. For further explanation on figure (C) refer to caption Fig. 6C. In upcurrent cores interglacial and glacial coarse-fraction distribution patterns are quite similar. During both periods sediments at proximal site 7 show a normal sorting pattern with decreasing percentages within each consecutive coarser grain size class. At more distal sites 8 and 9 a bimodal distribution pattern is evident indicating a deposition influenced by open ocean sedimentation at both sites.

within the 63–125 μm-fraction (approx. 32%). The fine sand-fraction shows relatively constant percentages between 24–28% along the whole transect. The medium sand content is lowest in proximal site 1 (17%), increases towards site 3 (30%) and varies around 30–32% in other sites situated further downslope. A similar spatial distribution pattern can be seen in the coarse sand-fraction. The very coarse sand-fraction shows no distinct changes along the entire offbank transect (0.9–1.9%).

The glacial sediments on average show a very similar distribution pattern for the subfractions along the entire offbank transect (Fig. 10B). All grain size distribution curves from the most proximal site 1 downslope to site 5 (1887 mbsl, 72 km offbank distance) show a dominance of the very fine to fine sand-fractions and decreasing percentages with increasing grain size classes.

A comparison of the interglacial and glacial averages (Fig. 10C) shows that the most obvious changes occur in the proximal sites 1 and 2 within the 63–125 μm and 250–500 μm-fraction. The glacial-to-interglacial difference within the fine sand-fraction (125–250 μm) is only minor (2–15%). The absolute percentages for the >1000 μm-fraction remain very low (0–2%) and very coarse sand-fraction only varies on a subordinate scale, therefore the large changes in the percentage as seen in Fig. 10 probably are a mathematical artifact.

3.4.4. Coarse-fraction subfractions in upcurrent sites

During interglacial periods the distribution pattern of the coarse subfraction at site 7 shows a dominance of fine sands. With increasing distance the percentage of the 63–125 μm and 125–250 μm-fraction decreases steadily (Fig. 11A). The very coarse sand-fraction (>1000 μm) displays only minor spatial changes. The averaged glacial distribution patterns shows a more bimodal distribution pattern (Sites 8 and 9) indicated by maximal percentages in the medium sand size and very fine sand size subclass (Fig. 11B).

4. Discussion

4.1. Long-term trends of mineralogical and grain size proxies

4.1.1. Neritic production

Neritic production is manifested in the sediment composition by the abundance of metastable carbonates like aragonite and HMC. Both can be used as proxies for sea level and sediment export, dissolution, and nutrients within the water column (Schwartz, 1996). Unfortunately the input of these components, such as aragonite, are controlled by more than one of the abovementioned factors, which hampers the unequivocal interpretation of these sedimentological and paleoceanographical proxies.

At present the facies distribution on Pedro Bank is controlled by (A) the production of biogenic material, and (B) the subdued, Pleistocene, subaerial, karstic, topography (Dolan, 1972). The platform top reaches up to sea level in the south and deepens to 40 m in the north. Four facies types were recognized on the platform top (Dolan, 1972): (1) Shallow reefs, restricted to the southern side of the platform, a facies type rich in components like coralline algae and encrusting foraminifera, (2) Reefal areas, rich in coral, *Halimeda*, and mixed reef biota, (3) Sand blanket facies, rich in pelletoids, rich in *Peneroplids* or mixed blanket; 68% of the platform top is covered by this facies type that contains molluscs, pelletoidal grains, and benthonic foraminifers, (4) Mud, a facies type that can be found in the deeper parts of the platform and on the slopes. Fines (<63 μm) are almost completely lacking on the platform top (Dolan, 1972) while wind-driven currents, with velocities of about 1.5 knots, preferentially remove this type of sediments (Glaser, 1991).

Large quantities of *Halimeda* and *Halimeda* bioherms have been observed on top of Pedro Bank (Dolan, 1972), and for banks west of Pedro Bank (Hallock et al., 1988; Hine et al., 1988). These green algae supply huge amounts of fine aragonite needles to the periplatform sediments. SEM studies of the bulk periplatform sediment showed the occurrence of fine aragonite needles as a major part of the matrix of the studied sediments (Andresen, 2000). The input of this fine (bank-derived) aragonite peaks at the beginning of interglacials within cores used for this study (Figs. 4 and 5). Thus, aragonite content mainly seems to be controlled by the flooding of the production sites, a pattern also found in sediment cores from Serranilla Basin (Duncan, 1997). Within cores from Pedro Channel an increase in aragonite contents was observed at the end of interglacials prior to MIS 5 (Schwartz, 1996). A possible explanation for this different pattern might be that all sediment cores from the northwestern margin of Pedro Bank are located within the main direction of sediment export from the shallow bank top (Glaser, 1991), whereas the sites studied by Schwartz (1996) are not situated in such a basinal position. In addition, dissolution by corrosive intermediate water masses (NADW vs. AAIW) might have modified the input signal (Haddad and Droxler, 1996; Schwartz, 1996). However, Droxler et al. (1991) showed that aragonite saturation at the NNR is reached at 1800 mbsl, and thus only might affect the aragonite signal in the deepest core studied (Site 6).

The content of fine HMC is an indicator for sea level fluctuations and/or preservation or dissolution of HMC (Haddad and Droxler, 1996; Schwartz, 1996). HMC originates from the production on the bank top or from fine cements formed at the seafloor (Schlager and James, 1978; Glaser and Droxler, 1993), and is more susceptible to dissolution at intermediate water depth than aragonite (Schlager and James, 1978; Walter and Morse, 1984). The long-term trends in the percentage of HMC shows distinct differences for the analyzed sites: (1) Shallow site 1 (648 mbsl) shows a long-term increase in maximum HMC percentages from MIS 8 to 1, (2) intermediate sites 2 to 4 (893–1023 mbsl) display no general long-term change, but a more or less clear interglacial/glacial cyclicity, whereas (3) sites from a depth exceeding 1445 mbsl (Sites 5, 6 and 9) display a long-term increase in the maximum HMC percentage since interglacial MIS 9 to the recent (Figs. 4 and 5).

The trend observed at proximal site 1 indicates a change within the production of HMC-organisms on top of Pedro Bank (i.e. a compositional change of biota or an enhanced preservation of metastable HMC since MIS 8 in shallow sediments of core 1). The sediments deposited in water depth between 893–1023 mbsl do not show any major variations or trends in the input of metastable carbonates. The depositional depth of these sites varies around 1100 mbsl, which is the upper level of partial dissolution of metastable carbonates observed in the basins on the NNR (Glaser and Droxler, 1993; Schwartz, 1996; Haddad and Droxler, 1996). Thus, it is unclear why the fine aragonite and fine HMC content do not show any distinct long-term trends as observed in a variety of other sediment cores from intermediate water depths on the NNR (Glaser and Droxler, 1993; Schwartz, 1996). However, at sites 2, 3, and 4 a similar cyclicity of the HMC signal is observed, which seems to correlate with the preservation/dissolution cycles described by Haddad and Droxler (1996) for intermediate water depths in the Caribbean Sea. Finally sediment cores deposited under full influence of intermediate and deep water masses (>1445 mbsl) exhibit a long-term increase in the maximum percentage of HMC, which clearly shows an increase in the preservation from MIS 9 to the recent interglacial, a trend also observed by Schwartz (1996).

4.1.2. Planktonic production — nutrients and current winnowing

Although fine calcite monitors the rain of coccoliths from the overlying photic zone, the content of fine LMC can be used as a proxy for changes in surface water productivity (=nutrients) and the evolution of current strength (=winnowing) (Schwartz, 1996). Glaser and Droxler (1993) stated that during the last 200 ky current velocities in Nicaraguan Rise channels increased during lowered sea levels due to the restriction of the seaways. Assuming a constant coccolith production (MacIntyre et al., 1976; Glaser and Droxler, 1993), lower glacial than interglacial percentages and accumulation rates in fine LMC could be explained by sediment winnowing. At nearly all sites, except for sites 2 and 4, which show no clear trend, a long-term decrease exists in the input of fine LMC (Figs. 4 and 5). This trend was also observed within shallow and deep sites from the Walton Basin (Glaser and Droxler, 1993), Pedro Channel (Schwartz, 1996) and Serranilla Basin (Duncan, 1997), and suggests increased current activity during the Late Brunhes Epoch (0–185 ky; Schwartz, 1996).

The coarse-fraction content shows a distinct trend: within sites 1 to 4 and 9, from shallow and intermediate water depths (648–1445 mbsl), an overall increase during the last 300 ky is observed (Figs. 4 and 5). The same trend was observed by Schwartz (1996) for sites from Pedro Channel and interpreted as a long-term increase in the availability of nutrients. Our study shows that most of the coarse-fraction of Pedro Channel sediments consists of planktonic foraminifera, and to a minor extent of pteropods (Fig. 3; Glaser and Droxler, 1993; Schwartz, 1996). Schwartz (1996) suggests that the accumulation and/or the percentage of the coarse-fraction can be considered as a qualitative proxy for surface water nutrient flux, as calcitic planktonic foraminifera are not subjected to dissolution or winnowing because of their size. Dilution by fine bank-derived neritic or siliciclastic input, as well as by the removal of fines due to current winnowing (Glaser and Droxler, 1991, 1993), might also play a role in modifying the relative percentages of the coarse-fraction.

4.1.3. Non-carbonate input — current transport

The abundance of non-carbonates shows a clear glacial–interglacial cyclicity with higher percentages during glacial MIS 2, 4, 6 and 8 (Figs. 4 and 5). An exception to this rule forms MIS event 7.4, an extreme sea level lowstand within interglacial MIS 7, with a sea level stand of about −80 mbsl (Haddad, 1994). At all sites a long-term increase in the content of fine non-carbonates was observed. Most of the non-carbonates originate from the large South American rivers like the Orinoco, Magdalena and Amazon. These rivers preferentially shed large amounts of sediment into the Atlantic Ocean and the Caribbean Sea during glacial periods (Reid et al., 1996; Schwartz, 1996; Flood and Piper, 1997; Franz, 1999). Increased current transport as also observed in the fine LMC record for the last 200 ky (Schwartz, 1996) might have been the main control

shaping the input patterns of non-carbonates (Duncan, 1997). This is also supported by the fact that higher percentages of non-carbonates are found at upcurrent sites that are located closer to the sources of non-carbonates, a pattern also evident in Serranilla Basin, west of Pedro Channel (Duncan, 1997).

4.2. Spatial variations in downcurrent site transect

4.2.1. Mineralogy

Aragonite displays, as expected, highest percentages in proximal sites and lowest at distal sites, and therefore shows the decreasing influence of the export of fine-grained neritic sediments with increasing distance from the carbonate bank (Figs. 6 and 12). Similar patterns have been described for the Bahamian carbonate slopes (Eberli et al., 1997; Rendle et al., 2000) and the basins surrounding Pedro Bank (Glaser and Droxler, 1991, 1993; Schwartz, 1996). This typical pattern is modified by the dissolution of metastable carbonates, from 1100 mbsl downwards during interglacials (Glaser and Droxler, 1993; Andresen, 2000). However, the spatial distribution pattern of aragonite, along the northwestern transect, shows that in the main direction of sediment export, the
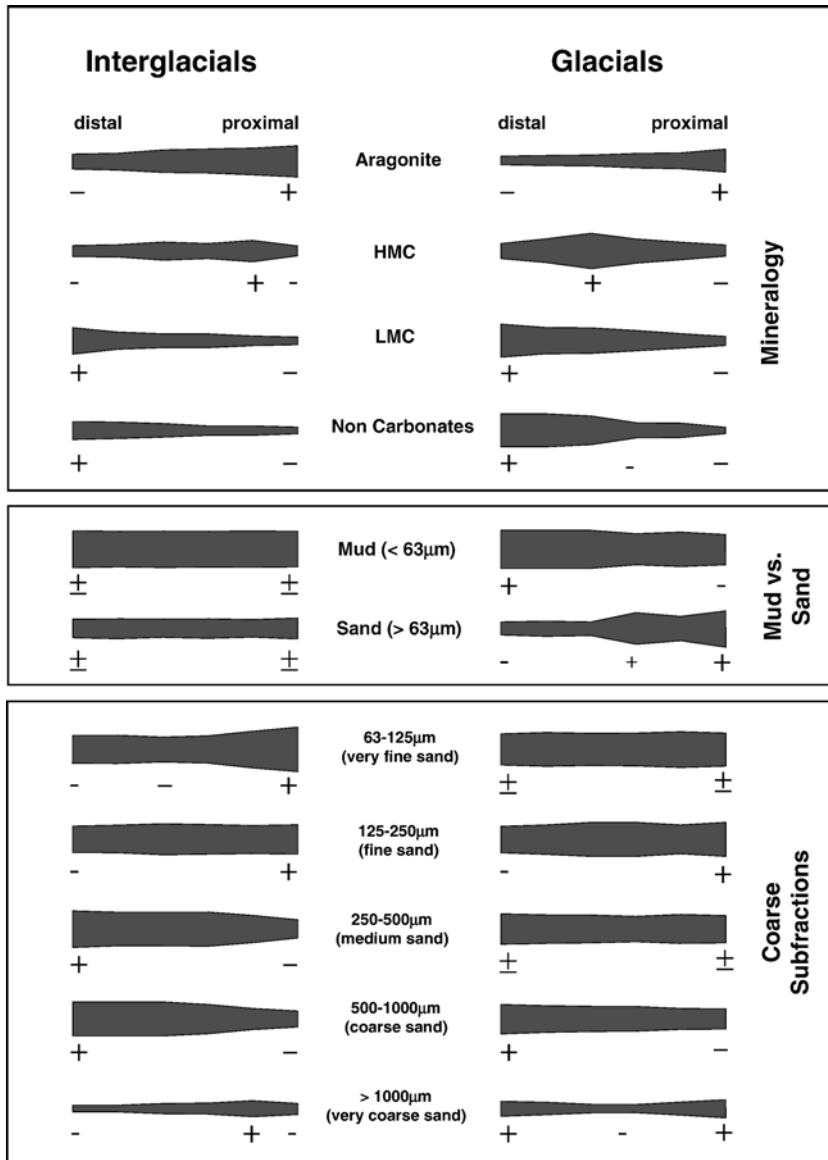

Fig. 12. General overview on spatial variations of mineralogical and grain size proxies along the downcurrent offbank transect. Bar thickness shows relative scale for interglacial and glacial proxy variations. Variations are based on data displayed within Figs. 6–11.

input of bank-derived aragonite exceeds the dissolution effects during interglacials.

HMC is an indicator for offbank transport at proximal sites and at the same time an indicator for dissolution of metastable carbonates in sediments deposited at intermediate water depths during interglacials. The exceptionally low average percentage during interglacials at site 7 might indicate (1) the low export potential of HMC biota, (2) the dilution of HMC by the high percentages of aragonite or (3) the existence of dissolution of calcium carbonate in the upper 500–1000 m of the ocean (Milliman et al., 1999). Both, interglacial and glacial percentages show a spatial increase with greater offbank distance along the transect, which culminates at about 1000 mbsl (site 4; Figs. 6 and 12). This pattern is more pronounced during glacials (Fig. 4F), either due to better preservation of HMC at intermediate water depths during these periods (Haddad and Droxler, 1996; Schwartz, 1996) or the existence of submarine HMC-cements, as observed by Glaser and Droxler (1993) in cores from Walton Basin, north of Pedro Bank. The apparent drop in HMC content at distal sites 5 and 6 (water depths exceeding 1880 mbsl; Fig. 6A and B) can be attributed to an increase in dissolution of metastable carbonates below 1800–2000 mbsl (Chen, 1968; Droxler et al., 1988).

The general increase of LMC during interglacials and glacials with greater offbank distance reflects the increasing pelagic, and decreasing neritic influence in the mineralogical sediment composition (Fig. 6A and B). The percentage of fine non-carbonates shows a similar pattern to LMC with a general percentage increase with greater offbank distance. During glacials this trend is more pronounced due to the preferential input of non-carbonates during these periods (Bowles and Fleischer, 1985; Glaser and Droxler, 1993; Schwartz, 1996).

4.2.2. Grain sizes

In previous studies grain size variations were primarily described from the siliciclastic environment and used to understand depositional processes and environments (Boggs, 1987 cum lit.). In carbonate environments grain size is only very broadly used in the Dunham (1962) classification. More recently, studies on the evolution of carbonate platforms used the grain composition, but not grain size, as an important source of information (e.g. Haak and Schlager, 1989; Reijmer et al., 1992).

Within the carbonate depositional realm the coarse-fraction content was mainly used in pelagic sediments to obtain knowledge on paleoceanographic changes in the ocean, such as changes in planktonic surface productivity (e.g. Lynts et al., 1973; Prell, 1978; Glaser and Droxler, 1993) or as an indicator for dissolution (Bassinot et al.,

1994). Only recently more information became available, at least on the content of coarse-fraction, for modern periplatform sediments from the Northern Nicaragua Rise periplatform environments (Triffleman et al., 1992; Glaser and Droxler, 1993; Schwartz, 1996; Duncan, 1997) and the Bahama Bank (Westphal et al., 1999; Rendle et al., 2000). These studies showed that during highstands in sea level (interglacials) most of the sediment export, preferentially of fine-grained sediments, takes place from the shallow-water carbonate banks, whereas lower accumulation is evident during glacials in the periplatform environment (Kendall and Schlager, 1981; Droxler and Schlager, 1985; Reijmer et al., 1988; Glaser and Droxler, 1993; Schlager et al., 1994; Schwartz, 1996; Duncan, 1997). The spatial evolution of the coarse-fraction and coarse subfraction contents shows the large influence of offbank transport on the periplatform sedimentation during interglacials and the impact of gravity-controlled sedimentation (and other paleoceanographical parameters) on the slopes of Pedro Bank during glacial times. This scenario ultimately results in the dominance of the fine fraction during interglacials, whereas during glacial sea level lowstands there is a tendency for deposition of coarser sediments, at least at proximal sites.

The coarse-fraction content along the northwestern offbank transect reveals no major changes during interglacial highstands in sea level (compare Figs. 8 and 12). This low spatial variation probably indicates the high export potential of fine-grained sediments from the downcurrent (leeward) margins of Pedro Bank (Glaser and Droxler, 1993) and the consistent (high) surface–water production of coarse pelagic components (Prell, 1978; Glaser and Droxler, 1993). These findings agree with those discussed by Hine et al. (1981a,b), Rendle et al. (2000) and Rendle-Bühring and Reijmer (2005) for the leeward bank margin of GBB, although the dominant factor for the dispersal of shallow-water sediments at the GBB is the main wind direction (Wilber et al., 1990). Within the study area, the Caribbean Current steers the sediment dispersal on the slopes and within the basins (Glaser and Droxler, 1993; Schwartz, 1996). The small differences that are evident in the coarse to fine fraction percentages along the transect (Figs. 10 and 12) might be modified by local factors such as the position of the sites relative to the platform, local topography (Andresen et al., 2003), or surface and bottom currents (Mullins et al., 1980). Other factors that might lead to a similar dominance of the fine fraction along the entire downcurrent transect are (1) resedimentation of fine fraction sediments from the upper slope or (2) offbank transport by "density cascading" as observed at the GBB (Wilson and Roberts, 1992, 1995).

Within the coarse-fraction itself a distinct change in the subdivisions occurs in a spatial context during the interglacials. Whereas in both proximal sites 1 and 2 normal sorting is evident (decrease in percentages of each coarser grain sized subdivision; Fig. 10A), this pattern changes at sites further downslope to a more bimodal distribution with maximum percentages in the very fine sand and medium sand-fraction (Fig. 10A). This shows the change from a generally bank-input controlled sedimentation at proximal sites to a mixed, neritic/pelagic sedimentation at distal basinal sites.

During glacial sea level lowstands the proximal sites (<30 km; sites 1 to 3) from 648–975 mbsl exhibit highest coarse-fraction contents of up to 34% (Site 1; Fig. 8B), while the distal sites (>40 km; Sites 4 to 6) show lowest glacial coarse-fraction percentages (Figs. 8 and 12). The concentration of coarse sediment is therefore more significant during glacials. The high percentage at the proximal site 1 can be mainly attributed to current winnowing and related removal of fine sediment constituents at this shallow site due to enhanced flow of the Caribbean Current (Glaser and Droxler, 1993). Aforementioned authors estimated that bottom currents have removed about 75% of the fines deposited during glacials above 600 mbsl, which explains the observed overall highest coarse-fraction content at site 1 located at 648 mbsl. A similar trend was also observed for Pliocene–Holocene slope deposits at the GBB (Rendle et al., 2000; Westphal et al., 1999).

Another major sedimentary process that could have caused the higher coarse-fraction contents within shallow and particularly proximal sites near Pedro Bank is erosion and reworking of upper slope deposits along with major trans- or regressions as well as during extended sea level lowstands (Shanmugan and Moiola, 1982, 1984; Cook and Mullins, 1983; Sarg, 1988; Cook and Taylor, 1991). Although this pattern is mainly observed in siliciclastic environments (Emery, 1996), it should not be neglected along carbonate slopes.

The irregular, tectonically derived seabottom morphology along the northwestern slope-to-basin transition at Pedro Bank (Andresen, 2000; Andresen et al., 2003) might enhance bypassing of coarser glacial deposits downslope as far as site 3 (±40 km). Foreslope research at the northwestern margin of Pedro Bank (Dullo, 1997; Andresen, 2000) shows that the morphology there most probably displays such a bypass slope. These types of bypass slopes also have been recognized along the GBB (Schlager and Ginsburg, 1981; Ginsburg et al., 1991; Grammer et al., 1993).

These reworking processes appear preferentially along with gravity-induced sediment transport. However-er, turbidites leave their coarser load further upslope, whereas in more distal parts of the basin, preferentially the fine endtails of turbidites are deposited (Eberli, 1991). The lithology and the composition of calciturbidites near Pedro Bank confirm this picture with prevailing fine-tail turbidites at distal sites 4, 5 (and 6). At sites further upslope, the grain composition shows a tendency to coarser grain sizes (Andresen, 2000).

The subdivisions of the coarse-fraction in glacials along the downcurrent transect displays a normal sorting pattern in almost all sites, i.e. decreasing content of each consecutive subfraction with increasing grain size. This indicates that similar depositional processes have been present at all sites, except for the most distal site 6 in central Pedro Channel, which shows a bimodal distribution with grain size maxima in the very fine sand and the medium sand-fraction. The latter is probably related to the different depositional environment within central Pedro Channel with different sediment sources. The peak of very fine sand probably reflects the input of fine neritic material and/or fine pelagic rain, whereas the peak in the medium sand-fraction can be attributed to the high input planktic foraminifera and pteropods, which are most common within the 250–500 μm-fraction.

Some general trends can be deduced comparing the leeward–windward, grain size distribution pattern observed at Great Bahama Bank (Rendle and Reijmer, 2002; Rendle-Bühring and Reijmer, 2005) and the downcurrent–upcurrent differences found at Pedro Bank. In both carbonate systems an increase in the distribution of coarser grains at the upcurrent (Pedro Bank) — windward margin (GBB) could be observed during interglacials. This results from the lower sediment export potential of the platform against the main current direction in both sedimentary systems. This difference results in dissimilar sediment transport processes at both platform margins, a productivity-export mode for the leeward/downcurrent margin versus a dominance of mass transport processes for the windward/upcurrent margin.

As grain size and mineralogy data of the sediments describe the nature of the periplatform sediments only to a certain extent, it is also important to obtain knowledge on the composition of the coarse grain fraction.

This is much more important in the carbonate environment, where grain sizes are also influenced by a "biological growth factor". To understand both datasets in the context of climate and sea level fluctuations it is necessary to know the origin of these grains (skeletal vs. non-skeletal, neritic vs. pelagic). Fig. 3 shows some differences between glacial and interglacial sediments that strengthen the grain size and mineralogy trends presented.

5. Conclusions

The analysis of several periplatform cores in the surrounding of Pedro Bank showed the presence of characteristic depositional environments during the last 300 ky.

The spatial distribution along the leeward, downcurrent margin shows a distinct pattern:

1. During *interglacial highstands in sea level* the fine sediment fraction (<63 μm) dominates periplatform sediments along the entire leeward, downcurrent transect without any spatial variations. The sediments are mainly of neritic origin preferentially fine aragonite needles. This dominance holds for distances up to 40 km from the margin. Further downslope aragonite is still the most abundant mineral, but the pelagic carbonate mineral content (LMC) increases. Within the subordinate coarse-fraction classes (>63 μm) the very fine sand-fraction dominates only at proximal sites (<20 km), due to the influence of fine neritic sediments shed offbank. More distal sites (>20 km) show a more bimodal distribution pattern in the coarse grain sizes with maximum percentages within the very fine and medium sand-fraction. This indicates a mixed neritic/pelagic signal.

2. During *glacial lowstands in sea level* a twofold division in the spatial distribution of the periplatform sediments is evident. A proximal environment (<28 km) with enhanced coarse-fraction percentages faces a distal environment (>28 km) with a strong dominance of the fine fraction (>90%). The raised coarse-fraction content at proximal sites is the result of various interacting processes: (1) lower input of fine neritic sediments, (2) increased current winnowing, and (3) redepositional processes at the upper slope during lowered sea level, and the export of this material to "proximal basinal" sites (<28 km). In the subordinate coarse-fraction classes a similar distribution pattern is found at all sites, showing a bimodal grain size distribution. This shows a low neritic influence within the coarse-fraction, and similar pelagic influence on the sedimentation at all sites during glacials.

At upcurrent sites no clear spatial distribution pattern is present. In general the mineralogy displays a similar spatial evolution as seen along the downcurrent margin, but with overall reduced percentages. This is due to the lower export potential of the platform against the main direction of the Caribbean Current, one important factor for neritic sediment dispersal in the study area. The coarse-fraction content is slightly higher during interglacials compared to the downcurrent margin, showing the main difference in sediment composition between the up- and downcurrent margin. This agrees with the patterns found for the leeward and windward margins of Great Bahama Bank (Rendle-Bühring and Reijmer, 2005). During glacials a similar reduction in the percentage of the coarse-fraction is evident in a spatial context. The percentage, however, is lower than at the proximal, downcurrent sites. This also substantiates the reduced sediment export and redeposition potential at the upcurrent margin.

Acknowledgements

Appendix A

A.1. Description of used methods

A.1.1. Stratigraphy — $\delta^{18}O$ and aragonite stratigraphy

The surface-dwelling planktic foraminfera *Globigerinoides sacculifer* (355–425 μm) was used for isotope analysis. At least 10 well-preserved specimens without the sac-like final chamber were selected (Duplessy et al., 1981) to avoid the isotopic signature from a deeper water mass.

The oxygen and carbon isotopes were measured on a FINNIGAN mass spectrometer ("Kiel CARBO II device") at GEOMAR. The stable oxygen and carbon isotopes were calibrated to a laboratory internal standard gas, and then calibrated against the NBS 19 carbonate standard of the National Bureau of Standards (PDB-Standard; Craig, 1957). The overall reproducibility of measurements (±1 s) averages 0.03‰ for $\delta^{18}O$ (and 0.01‰ for $\delta^{13}C$) referred to a laboratory internal standard (Solnhofener Plattenkalk).

A.1.2. Stratigraphy — aragonite variations with time as a proxy for $\delta^{18}O$ ("Aragonite stratigraphy")

Extensive export of metastable aragonite sediments from carbonate platforms into the periplatform

environment mainly occurs during highstands in sea level, when bank tops are flooded, whereas lower aragonite contents, and thus reduced export, are observed during lowstands in sea level, when the platforms are exposed. This highstand shedding pattern has been observed along the Bahama Platform (Droxler et al., 1983; Droxler and Schlager, 1985; Reijmer et al., 1988; Rendle, 2000) as well as many other platforms like the Maldives and the Northern Nicaragua Rise (e.g. Boardman et al., 1986; Droxler et al., 1990; Glaser and Droxler, 1993). Aforementioned authors clearly demonstrated the correlation between the percentage of fine aragonite in periplatform sediments and the $\delta^{18}O$ record in periplatform sediments. Glaser and Droxler (1993) showed that this also applies for sediments from Walton Basin north of Pedro Bank. This close correlation justifies the use of aragonite variations with time as a proxy for $\delta^{18}O$ variations, when no oxygen isotope data are available. This method was applied to cores M35048-1 (648 mbsl) and PC059 (1887 mbsl).

A.1.3. Stratigraphy — age models and correlation of the oxygen isotopes to the SPECMAP-Stack

By pattern matching of the isotope or aragonite signatures of each core against the SPECMAP stacked isotope curve of Imbrie et al. (1984) the sediments were dated relatively to the events of the SPECMAP curve. Data from Glaser and Droxler (1993), Schwartz (1996) and Duncan (1997) from the nearby Walton and Serranilla Basin and Pedro Channel were used to define specific isotope events. The actual correlation was made using the computer program "AnalySerie" (Paillard et al., 1996). This program calculates the "SPECMAP-age" by linear interpolation, which results in relative ages for all given depths of the analyzed cores. The correlation coefficient between the oxygen isotope curves of cores (or other proxies used) in this study and the SPECMAP curve are good ($r^2 = 0.9$).

A.1.4. Stratigraphy – biostratigraphy (Globorotalia menardii complex)

The *G. menardii* complex stratigraphy was determined for all cores by visual inspection of the subfractions 250–500 µm, 500–1000 µm and >1000 µm to prove the presence or absence of the two Globorotaliid species, *G. menardii* and *G. tumida* (Globorotaliid abundance). The following categories were used "no presence, minor presence, common, frequent", which agree with those of other studies in the Caribbean (Ericson and Wollin, 1968; Prell and Hays, 1976; Glaser and Droxler, 1993; Haddad, 1994). This biostratigraphic tool can be used to support isotope stratigraphic interpretations. The zones of presence

and absence start with the letter Z (=Holocene) and then count back in time (see Fig. 2; Ericson and Wollin, 1956).

A.1.5. Stratigraphy – radiocarbon ages (AMS ^{14}C-dating)

Radiocarbon dating (AMS ^{14}C-dating) was applied to 9 Holocene and MIS 3 samples with a slight preference for samples from marine oxygen isotope stage 3. Mixed sediment samples (preferentially planktic foraminifera and pteropods) of the 250–500 µm or the 355–425 µm-fraction were used. These samples were identical to those used for oxygen isotope analysis. No monospecies samples were measured.

The Leibniz Laboratory at the Christian-Albrechts-University in Kiel provided radiocarbon analysis. The dates are corrected "conventional ages" according to Stuiver and Pollach (1977). The global 400-yr reservoir age correction was not applied. The AMS ^{14}C-data were solely used to confirm the ages obtained from the linear interpolation of the oxygen isotope data with the SPECMAP stack, and in general to support the interpretation of stage 3 samples as obtained from the oxygen isotope curve. Fig. 2 displays two stratigraphic columns for cores M35049 and PC059, showing the $\delta^{18}O$ or the aragonite stratigraphy, biostratigraphy and radiocarbon ages, in their stratigraphic context.

A.1.6. Mineralogy – calcium carbonate and organic carbon content

The measurements of the total carbon content (TC) and total organic carbon content (TOC) were performed on a Carlo Erba CHNO Analyser NA1500 at GEOMAR (Kiel, Germany).

During one automated run of 50 samples four blank containers, seven standard samples (0.1–1.0 mg of "acetanilide standard" for samples with high $CaCO_3$ content) and one internal standard with a known percentage of carbon (3.75% TC) were analyzed. The blanks and standards were used to produce a calibration curve that finally results in the TC- and TOC-content of the sample. Each sample was measured twice. If both samples differed more than 0.2% for TC or 0.1% for TOC, the sample was remeasured. Assuming that all inorganic carbon (IC) is bound in calcium carbonate, the weight percentages of calcium carbonate was calculated using the following formula

$$CaCO_3(weight\%) = IC(weight\%) \times 8.3333$$
$$with \quad IC = TC - TOC.$$

A standard deviation of 0.11% for 25 standard measurements of an internal standard (sample SO-109) circumstantiates the availability of the method.

A.1.7. Mineralogy – X-ray powder diffraction (XRD)

X-ray diffraction was used to analyze the carbonate mineralogical composition of bulk sediment as well as the fine fraction. The peak area method (Milliman, 1974), that is the integration of counts under a given peak, provides the best estimate of the content of a known or unknown mineral.

Using a Phillips X-ray machine (PW 1710) at GEOMAR Kiel the relative abundance of the carbonate phases (aragonite, low-magnesium calcite [LMC] and high-magnesium calcite [HMC]), as well as quartz, an indicator for terrigenous input, was measured. A Co-Ka-Anode was used with a wavelength of 1.7903 Å at 40 kV and 35 mA. Each sample was oven-dried at 40 °C and ground in a mortar by hand not longer than 3 min to produce sediment with a grain size less than 63 μm. This procedure was used to avoid measurement artifacts that originate from inhomogeneous particle size and transformations of aragonite to LMC due to overgrinding (Milliman, 1974). Each sample was pressed into an aluminum holder and scanned with a speed of 0.01°/s within the range of 25°–40° 2-theta. This range covers all main X-ray diffraction peaks of the minerals of interest.

The relative percentages of the carbonate minerals were calculated using an in-house calibration curve which used known weight percentages of mixtures from pure skeletal aragonite (Red Sea coral) and pure synthetic calcite. Each calibration sample was measured three times. After each individual measurement of a sample it was disposed, and a new sample was prepared. The resulting standard deviation of these 3 measurements shows a linear increase from 0.08 to 5.16% 2 s with increasing aragonite percentage (Emmermann et al., 1999).

The carbonate mineralogical data are calculated percentages of the fine carbonate component within the bulk sediment (which therefore do not add up to 100%). This calculation was established by Glaser and Droxler (1991) and Neumann and Land (1975), as the main portion of neritic material of the carbonate platforms is exported as fine aragonite. Therefore this calculation shows a clearer signal of the neritic input, undiluted from planktonic input.

The carbonate mineralogical data were determined using the following equation:

$$\text{Carbonate component}_{(\text{in bulk sediment})}$$
$$= \text{Carbonate component}_{(\text{raw data in percent})}$$
$$\times \text{ Carbonate content ratio}_{(\text{fine fraction})}$$
$$\times \text{fine fraction ratio}$$

with

$$\text{Carbonate content ratio}_{(\text{fine fraction})} = CaCO_3 \: / \: 100$$
$$\text{fine fraction ratio} = \text{Fine fraction percentage} \: / \: 100.$$

A.1.8. Grain size analysis — pre-sieving procedures

Fresh or constantly cooled bulk sediment samples were vacuum freeze-dried at about −40 °C. These dehydrated samples were weighed to a precision of 0.001 g. Before starting wet-sieving, the samples were treated with demineralized water for a few hours to one day to deflocculate the dried sample again and thus ease the wet-sieving process.

A.1.9. Grain size analysis — wet-sieving

Using the suspended bulk sediment sample, the wet-sieving procedure separates clay and silt-sized particles (<63 μm) from the sand sized fraction and coarser particles (>63 μm). This is achieved by washing the suspended sediment through a 63 μm standard sieve with demineralized water. The fine sediment is collected in 1–3 l bottles in which it settles down within a few days or weeks (depending on the clay and silt-size distribution). After settling, the water is removed carefully and the fine fraction is dried at 40 °C.

A.1.10. Grain size analysis — dry sieving

The dried and weighted coarse-fraction samples (>63 μm) were split into five subfractions using the Wentworth–Udden grain size scale (Wentworth, 1922): very fine sand: 63–125 μm; fine sand: 125–250 μm; medium sand: 250–500 μm; coarse sand: 500–1000 μm; and very coarse sand to rubble: >1000 μm. The weight percentages of each subfraction was determined as part of the total coarse-fraction weight.

A variety of selected coarse-fraction photographs containing typical planktic, benthic and shallow-water originated biota is shown in Fig. 3.

References

Andresen, N., 2000. Sediment composition of periplatform sediments and calciturbidites around Pedro Bank, southwestern Caribbean Sea. Unpublished PhD thesis, Christian-Albrechts-Universität, Kiel, Germany.

Andresen, N., Reijmer, J.J.G., Droxler, A.W., 2003. Timing and distribution of calciturbidites around a deeply submerged carbonate platform in a seismically active setting (Pedro Bank, Northern Nicaragua Rise, Caribbean Sea). International Journal of Earth Sciences 92, 573–592.

Bassinot, F.C., Labeyrie, L.D., Vincent, E., Quidelleur, X., Shackleton, N.J., Lancelot, Y., 1994. The astronomical theory of climate and the age of the Brunhes-Matuyama magnetic reversal. Earth and Planetary Science Letters 126, 91–108.

Boardman, M.R., Neumann, A.C., Baker, P.A., Dunlin, L.A., Kenter, R.J., Hunter, G.E., Kiefer, K.B., 1986. Banktop responses to Quaternary fluctuations in sea level recorded in periplatform sediments. Geology 14, 28–31.

Boggs, S.J., 1987. Chapter 5: sedimentary textures. Principles of Sedimentology and Stratigraphy 105–122.

Bowles, F.A., Fleischer, P., 1985. Orinoco and Amazon river sediment input to the eastern Caribbean basin. Marine Geology 68, 53–72.

Chappell, J., Omura, A., Ezat, T., McCulloch, M., Pandolfi, J., Ota, Y., Pillans, B., 1996. Reconciliation of late Quaternary sea levels derived from coral terraces at Huon Peninsula with deep-sea oxygen isotope records. Earth and Planetary Science Letters 141, 227–236.

Chen, C., 1968. Pleistocene pteropods in pelagic sediments. Nature 219, 1145–1149.

Cook, H.E., Mullins, H.T., 1983. Basin margin. In: Scholle, P.A., Bebout, D.G., Moore, C.H. (Eds.), Carbonate Depositional Environments. American Association of Petroleum Geologists, Bulletin, vol. 11, pp. 539–619.

Cook, H.E., Taylor, M.E., 1991. Carbonate slope failures as indicators of sea level lowerings. American Association of Petroleum Geologists, Bulletin 75, 556.

Craig, H., 1957. Isotopic standards for carbon and oxygen correction factors for mass spectrometric analysis of CO_2. Geochimica Cosmochimica Acta 12, 133–149.

Dolan, P., 1972. Genesis and distribution of recent sediments on the Pedro Bank, south of Jamaica. Unpublished Ph.D. thesis, University College, London.

Droxler, A.W., Schlager, W., 1985. Glacial versus interglacial sedimentation rates and turbidite frequency in the Bahamas. Geology 13, 799–802.

Droxler, A.W., Schlager, W., Whallon, C.C., 1983. Quaternary aragonite cycles and oxygen isotope record in Bahamian carbonate ooze. Geology 11, 235–239.

Droxler, A.W., Morse, J.W., Kornicker, W.A., 1988. Controls on carbonate mineral accumulation in Bahamian basins and adjacent Atlantic ocean sediments. Journal of Sedimentary Petrology 58, 120–130.

Droxler, A.W., Haddad, G.A., Mucciarone, D.A., Cullen, J.L., 1990. Pliocene–Pleistocene aragonite cyclic variations in holes 714A and 716B (the Maldives) compared with Hole 633A (the Bahamas): records of climate-induced $CaCO_3$ preservation at intermediate water depths. Proceedings of the Ocean Drilling Program, Scientific Results 115, 539–567.

Droxler, A.W., Morse, J.W., Glaser, K.S., Haddad, G.A., Baker, P.A., 1991. Surface sediment carbonate mineralogy and water column chemistry: Nicaragua Rise vs. Bahamas. Marine Geology 100, 277–289.

Dullo, W.-C., 1997. Die Plattformhangmorphologie der Pedro Bank in der Karibik: geologisches Blatt NO-Bayern, vol. 47, pp. 303–320.

Duncan, D.S., 1997. The geologic and paleoceanographic evolution of the Serranilla Basin: Northern Nicaragua Rise, Caribbean Sea. Unpublished Ph.D. thesis, University of South Florida, Coral Gables, U.S.A.

Dunham, R., 1962. The classification of carbonate rocks according to depositional texture. In: Ham, W.E. (Ed.), Classification of Carbonate Rocks — A symposium. American Association of Petroleum Geologists Memoir, vol. 1, pp. 108–121.

Duplessy, J.C., Be, A.W.H., Blanc, P.L., 1981. Oxygen and carbon isotopic composition and biogeographic distribution of planktonic foraminifera in the Indian Ocean. Palaeogeography, Palaeoclimatology, Palaeoecology 33 (1–3), 9–46.

Eberli, G.P., 1991. Calcareous turbidites and relationship to sea-level fluctuations and tectonism. In: Einsele, G., Ricken, W., Seilacher, A. (Eds.), Cycles and Events in Stratigraphy. Springer Verlag, Berlin, pp. 340–359.

Eberli, G.P., Swart, P.K., Malone, M.J., 1997. Proceedings of the ocean drilling program. Initial Reports, vol. 166. ODP, College Station, Texas. 850 pp.

Emery, D., 1996. Carbonate systems. In: Emery, D., Myers, K.J. (Eds.), Sequence Stratigraphy. Cambridge University Press, Cambridge, England, pp. 211–237.

Emmermann, P., Reijmer, J.J.G., Andresen, N., 1999. Sedimentation rates of Quaternary periplatform sediments based on aragonite/calcite ratios: Sudanese Red Sea vs. Pedro Bank, Caribbean. In: Bruns, P., Haas, C. (Eds.), On the determination of sediment accumulation rates. Trans Tech Publications, Zürich, Switzerland, pp. 67–86.

Ericson, D.B., Wollin, G., 1956. Micropaleontological and isotopic determinations of Pleistocene climates. Micropaleontology 2, 257–270.

Ericson, D.B., Wollin, G., 1968. Pleistocene climates and chronology in deep-sea sediments. Science 162, 1227–1234.

Flood, R.D., Piper, D.J.W., 1997. Amazon Fan Sedimentation: the Relationship to Equatorial Climate Change, Continental Denudation, and Sea-level Fluctuations. In: Flood, R.D., Piper, D.J.W., Klaus, A., Peterson, L.C. (Eds.), Proceedings of the Ocean Drilling Program, Scientific Results, vol. 155. College Station, Texas, pp. 653–675.

Franz, S.O., 1999. Pliozäne Zeitreihen zur Rekonstruktion der Tiefenwasserzirkulation und der siliziklastischen Amazonasfracht im Äquatorialen Westatlantik (Ceara Schwelle, ODP Leg 154). Unpublished Ph.D. thesis, Christian-Albrechts Universität, Kiel, Germany.

Ginsburg, R.N., Harris, P.M., Eberli, G.P., Swart, P.K., 1991. The growth potential of a bypass marginm, Great Bahama Bank. Journal of Sedimentary Petrology 61, 976–987.

Glaser, K.S., 1991. Late Quaternary periplatform sediments and environments on the Northeastern Nicaragua Rise, Caribbean Sea. Unpublished Ph.D. thesis, Rice University, Houston, U.S.A.

Glaser, K.S., Droxler, A.W., 1991. High production and highstand shedding from deeply submerged carbonate banks, Northern Nicaragua Rise. Journal of Sedimentary Petrology 61 (1), 128–142.

Glaser, K.S., Droxler, A.W., 1993. Controls and development of Late Quaternary periplatform carbonate stratigraphy in Walton Basin (Northeastern Nicaragua Rise, Caribbean Sea). Paleoceanography 8, 243–274.

Grammer, G.M., Ginsburg, R.N., Harris, P.M., 1993. Timing of deposition, diagenesis, and failure of steep carbonate slopes in response to a high-amplitude/high-resolution fluctuation in sea level, Tongue of the Ocean, Bahamas. In: Loucks, R.G., Sarg, J.F. (Eds.), Carbonate Sequence Stratigraphy: Recent Developments and Applications. American Association of Petroleum Geologists Memoir, vol. 57, pp. 107–131.

Haak, A.B., Schlager, W., 1989. Compositional variations in calciturbidites due to sea-level fluctuations, late Quaternary, Bahamas. Geologische Rundschau 78, 477–486.

Haddad, G.A., 1994. Calcium carbonate dissolution patterns at intermediate water depths of the tropical oceans during the past Quaternary. Unpublished Ph.D. thesis, Rice University, Houston, U.S.A.

Haddad, G.A., Droxler, A.W., 1996. Metastable $CaCO_3$ dissolution at intermediate water depths of the Caribbean and western North Atlantic: implications for intermediate water circulation during the past 200.000 years. Paleoceanography 11, 701–716.

Hallock, P., Hine, A.C., Vargo, G.A., Elrod, J.A., Jaap, W., 1988. Platforms of the Nicaragua Rise: examples of the sensitivity of carbonate sedimentation to excess trophic sources. Geology 16, 1104–1107.

Hine, A.C., Wilber, R.J., Bane, J.M., Neumann, A.C., Lorenson, K.R., 1981a. Offbank transport of carbonate sands along open, leeward bank margins: northern Bahamas. Marine Geology 42, 327–348.

Hine, A.C., Wilber, R.J., Neumann, A.C., 1981b. Carbonate sand bodies along contrasting shallow bank margins facing open seaways in northern Bahamas. American Association of Petroleum Geologists Bulletin 65, 261–290.

Hine, A.C., Hallock, P., Harris, M.W., Mullins, H.T., Belknap, D.F., Jaap, W.C., 1988. Halimeda bioherms along an open seaway: Miskito Channel, Nicaraguan Rise, SW Caribbean Sea. Coral Reefs 6 (3–4), 173–178.

Imbrie, J., Hays, J.D., Martinson, D.G., McIntyre, A., Mix, A.C., Morley, J.J., Pisias, N.G., Prell, W.L., Shackleton, N.J., 1984. The Orbital Theory of Pleistocene Climates: Support from a Revised Chronology of the Marine δ^{18}O Record. In: Berger, A.L., et al. (Ed.), Milankovitch and Climate, Part, vol. I. D. Reidel Publishing Company, Dordrecht, The Netherlands, pp. 269–305.

Kendall, C.G.S.C., Schlager, W., 1981. Carbonates and relative changes in sea level. Marine Geology 44, 181–212.

Lynts, G.M., Judd, J.B., Stehmann, C.F., 1973. Late Pleistocene history of Tongue of the Ocean, Bahamas. Geological Society of America Bulletin 84, 2665–2684.

MacIntyre, A., Kipp, N.G., Be, A.W.H., Crowley, T., Kellog, T., Gardner, J.V., Prell, W.L., Ruddiman, W.F., 1976. Glacial North Atlantic 18.000 years ago: a CLIMAP reconstruction. In: Cline, R.M., Hays, J.D. (Eds.), Investigation of Late Quaternary Paleoceanography and Paleoclimatology. Geological Society of America Memoir, vol. 145, pp. 43–76.

Milliman, J.D., 1974. Marine Carbonates. Springer Verlag, Berlin. 375 pp.

Milliman, J.D., Troy, P.J., Balch, W.M., Adams, A.K., Li, Y.-H., Mackenzie, F.T., 1999. Biologically mediated dissolution of calcium carbonate above the chemical lysocline? Deep-Sea Research I (46), 1653–1669.

Mullins, H.T., Neumann, A.C., Wilber, R.J., Hine, A.C., Chinburg, S.J., 1980. Carbonate sediment drifts in northern Straits of Florida. American Association of Petroleum Geologists Bulletin 64, 1701–1717.

Neumann, A.C., Land, L.S., 1975. Lime mud deposition and calcareous algae in the Bight of Abaco, Bahamas: a budget. Journal of Sedimentary Petrology 45 (4), 763–786.

Paillard, D., Labeyrie, L., Yiou, P., 1996. Analyserie 1.07a PPC, Macintosh program performs time-series analysis. EOS Transactions 77, 379.

Prell, W.L., 1978. Upper Quaternary sediments of the Colombia Basin; spatial and stratigraphic variation. Geological Society of America Bulletin 89, 1241–1255.

Prell, W.L., Hays, J.D., 1976. Late Pleistocene faunal and temperature patterns of the Colombia Basin, Caribbean Sea. In: Cline, R.M., Hays, J.D. (Eds.), Investigation of Late Quaternary Paleoceanography and Paleoclimatology. Geological Society of America Memoir, vol. 145, pp. 201–220.

Reid, R.P., Carey, S.N., Ross, D.R., 1996. Late Quaternary sedimentation in the Lesser Antilles island arc. Geological Society of America Bulletin 108, 78–100.

Reijmer, J.J.G., Schlager, W., Droxler, A.W., 1988. Site 632: Pliocene–Pleistocene Sedimentation Cycles in a Bahamian Basin. In: Austin, J.A.J., Schlager, W. (Eds.), Proceedings of the Ocean Drilling Program, Scientific Results, vol. 166. College Station, Texas, pp. 213–220.

Reijmer, J.J.G., Schlager, W., Bosscher, H., Beets, C.J., McNeill, D.F., 1992. Pliocene/Pleistocene platform facies transition recorded in calciturbidites (Exuma Sound, Bahamas). Sedimentary Geology 78, 171–179.

Rendle, R.H., 2000. Quaternary slope development and sedimentology of the western, leeward margin of Great Bahama Bank (ODP Leg

166). Unpublished Ph.D. thesis, Christian-Albrechts-Universität, Kiel, Germany.

Rendle, R.H., Reijmer, J.J.G., 2002. Quaternary slope development of the western, leeward margin of the Great Bahama Bank. Marine Geology 185, 143–164.

Rendle, R.H., Reijmer, J.J.G., Kroon, D., Henderson, G.M., 2000. Mineralogy and Sedimentology of the Pleistocene to Holocene on the Leeward Margin of Great Bahama Bank. In: Swart, P.K., Eberli, G.P., Malone, M.J., Sarg, J.F. (Eds.), Proceedings of the Ocean Drilling Program, Scientific Results, vol. 166. College Station, Texas, pp. 61–76.

Rendle-Bühring, R.H., Reijmer, J.J.G., 2005. Controls on grain-size patterns in periplatform carbonates: marginal setting versus glacio-eustacy. Sedimentary Geology 175, 99–113.

Sarg, J.F., 1988. Carbonate Sequence Stratigraphy. In: Wilgus, C.K., Hastings, B.S., Kendall, C.G.S.C., Posamentier, H.W., Ross, C.A., Van Wagoner, J.C. (Eds.), Sea Level Changes — an Integrated Approach, vol. 42. SEPM Special Publication, pp. 155–181.

Schlager, W., Ginsburg, R.N., 1981. Bahama carbonate platforms — the deep and the past. Marine Geology 44, 1–24.

Schlager, W., James, N.P., 1978. Low-magnesian calcite limestones forming at the deep-sea floor, Tongue of the Ocean, Bahamas. Sedimentology 25, 675–702.

Schlager, W., Reijmer, J.J.G., Droxler, A.W., 1994. Highstand shedding of carbonate platforms. Journal of Sedimentary Research B64, 270–281.

Schwartz, J.P., 1996. Late Quaternary periplatform sediments and paleoenvironmental analysis of Pedro Channel, Northeastern Nicaragua Rise, Caribbean Sea. Unpublished M.Sc. thesis. Rice University, Houston, U.S.A.

Shanmugan, G., Moiola, R.J., 1982. Eustatic control of turbidites and winnowed turbidites. Geology 10, 231–235.

Shanmugan, G., Moiola, R.J., 1984. Eustatic control of calciclastic turbidites. Marine Geology 56, 273–278.

Stuiver, M., Pollach, H., 1977. Discussion: reporting of ^{14}C data. Radiocarbon 19 (3), 355–363.

Triffleman, N.J., Hallock, P., Hine, A.C., 1992. Morphology, sediments, and depositional environments of a small carbonate platform: Serranilla Bank, Nicaraguan Rise, Southwest Caribbean Sea. Journal of Sedimentary Research 62, 591–606.

Walter, L.M., Morse, J.W., 1984. Reactive surface area of skeletal carbonates during dissolution; effect of grain size. Journal of Sedimentary Petrology 54, 1081–1090.

Wentworth, C.K., 1922. A scale of grade and class terms for clastic sediments. Journal of Geology 30, 377–392.

Westphal, H., Reijmer, J.J.G., Head, M.J., 1999. Input and Diagenesis of a Carbonate Slope (Bahamas): Response to Morphology Evolution and Sea Level Fluctuations. In: Harris, P.M., Saller, A.H., Simo, T., Handford, R. (Eds.), Advances in Carbonate Sequence Stratigraphy – Application to Reservoirs, Outcrops, and Models, vol. 63. SEPM Special Publication, pp. 247–274.

Wilber, R.J., Milliman, J.D., Halley, R.B., 1990. Accumulation of bank-top sediment on the western slope of Great Bahama Bank: rapid progradation of a carbonate megabank. Geology 18, 970–974.

Wilson, P.A., Roberts, H.H., 1992. Carbonate-periplatform sedimentation by density flows: a mechanism for rapid off-bank and vertical transport of shallow-water fines. Geology 20, 713–716.

Wilson, P.A., Roberts, H.H., 1995. Density cascading: off-shelf sediment transport, evidence and implications, Bahama Bank. Journal of Sedimentary Research A65, 45–56.